

Supplementary Materials

Spectra–Structure Correlations in Isotopomers of Ethanol (CX_3CX_2OX ; $X = H, D$): Combined Near-Infrared and Anharmonic Computational Study

Krzysztof B. Beć ^{1,2,*}, Justyna Grabska ¹, Christian W. Huck ¹, and Mirosław A. Czarnecki ²

¹ Institute of Analytical Chemistry and Radiochemistry, Leopold-Franzens University, Innrain 80/82, CCB-Center for Chemistry and Biomedicine, 6020-Innsbruck, Austria; Justyna.Grabska@uibk.ac.at (J.G.); Christian.W.Huck@uibk.ac.at (C.W.H.)

² Faculty of Chemistry, University of Wrocław, F. Joliot-Curie 14, 50-383 Wrocław, Poland; mirosław.czarnecki@chem.uni.wroc.pl

* Correspondence: Krzysztof.Bec@uibk.ac.at; Tel.: +43-512-507-5783

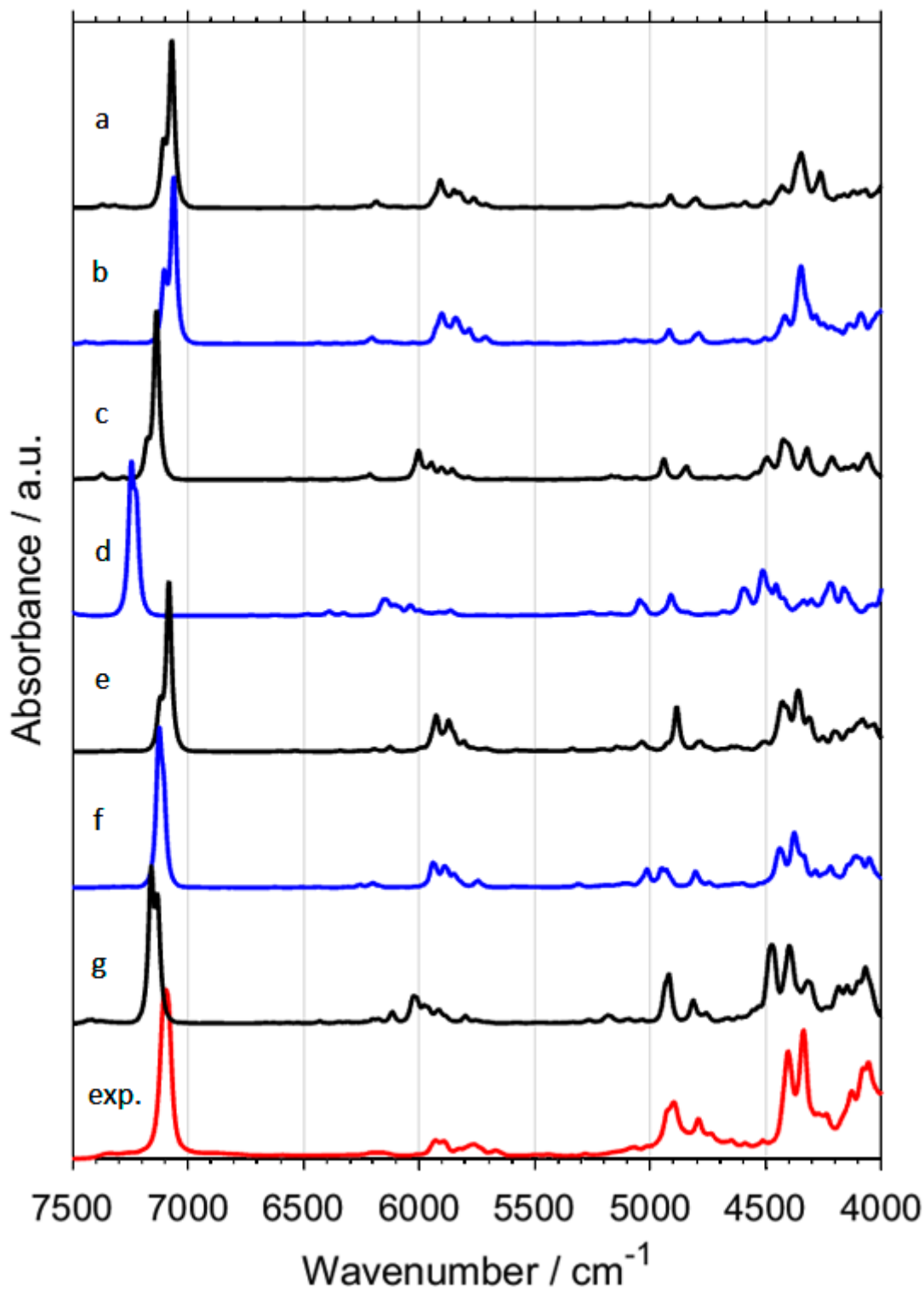
I. Figures

Figure S1. NIR spectra of $\text{CH}_3\text{CD}_2\text{OH}$ calculated with GVPT2 method at different levels of electronic theory; (a) B3LYP-GD3BJ/6-31G(d,p); (b) B3LYP-GD3BJ/6-31G(d,p)//CPCM; (c) B2PLYP-GD3BJ/6-31G(d,p)//CPCM; (d) MP2/6-31G(d,p)//CPCM; (e) B3LYP-GD3BJ/SNST//CPCM; (f) B2PLYP-GD3BJ/def2-TZVP//CPCM; (g) MP2/aug-cc-pVTZ//CPCM. Experimental spectrum (exp.) of $\text{CH}_3\text{CD}_2\text{OH}$ in CCl_4 (0.1 M).

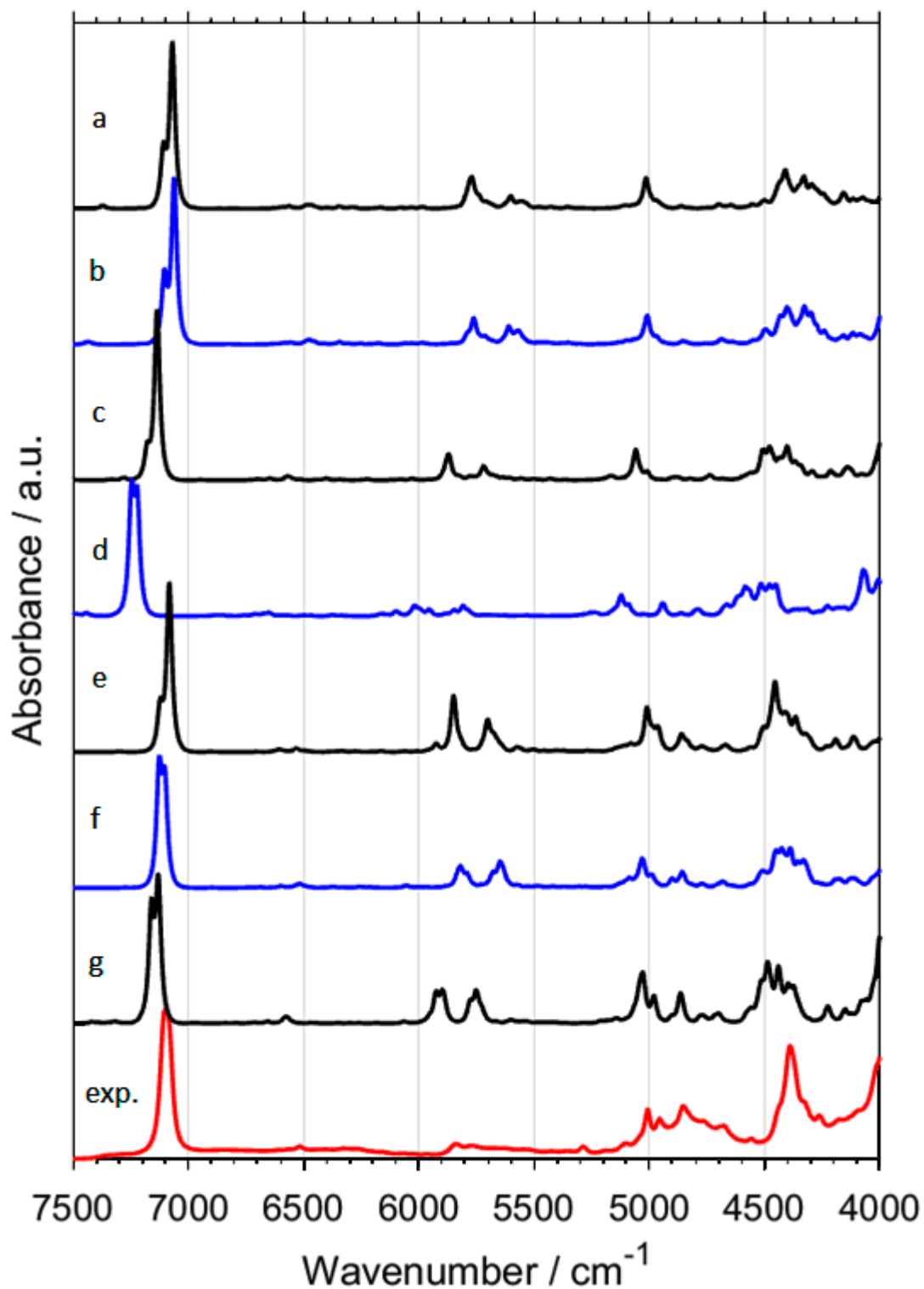


Figure S2. NIR spectra of $\text{CD}_3\text{CH}_2\text{OH}$ calculated with GVPT2 method at different levels of electronic theory; (a) B3LYP-GD3BJ /6-31G(d,p); (b) B3LYP-GD3BJ /6-31G(d,p)//CPCM; (c) B2PLYP-GD3BJ/6-31G(d,p)//CPCM; (d) MP2/6-31G(d,p)//CPCM; (e) B3LYP-GD3BJ/SNST//CPCM; (f) B2PLYP-GD3BJ/def2-TZVP//CPCM; (g) MP2/aug-cc-pVTZ//CPCM. Experimental spectrum (exp.) of $\text{CD}_3\text{CH}_2\text{OH}$ in CCl_4 (0.1 M).

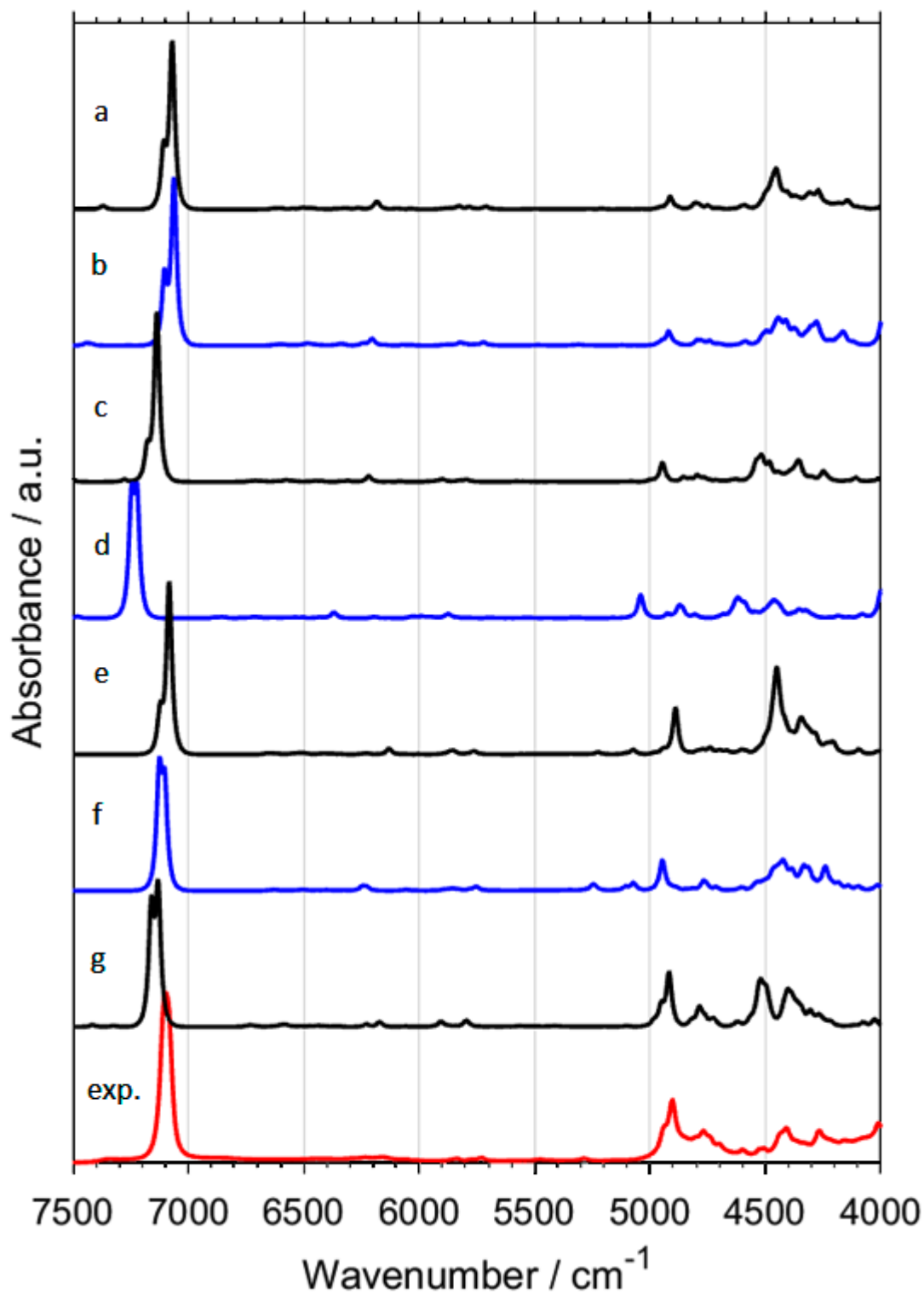


Figure S3. NIR spectra of $\text{CD}_3\text{CD}_2\text{OH}$ calculated with GVPT2 method at different levels of electronic theory; (a) B3LYP-GD3BJ /6-31G(d,p); (b) B3LYP-GD3BJ /6-31G(d,p)//CPCM; (c) B2PLYP-GD3BJ/6-31G(d,p)//CPCM; (d) MP2/6-31G(d,p)//CPCM; (e) B3LYP-GD3BJ/SNST//CPCM; (f) B2PLYP-GD3BJ/def2-TZVP//CPCM; (g) MP2/aug-cc-pVTZ//CPCM. Experimental spectrum (exp.) of $\text{CD}_3\text{CD}_2\text{OH}$ in CCl_4 (0.1 M).

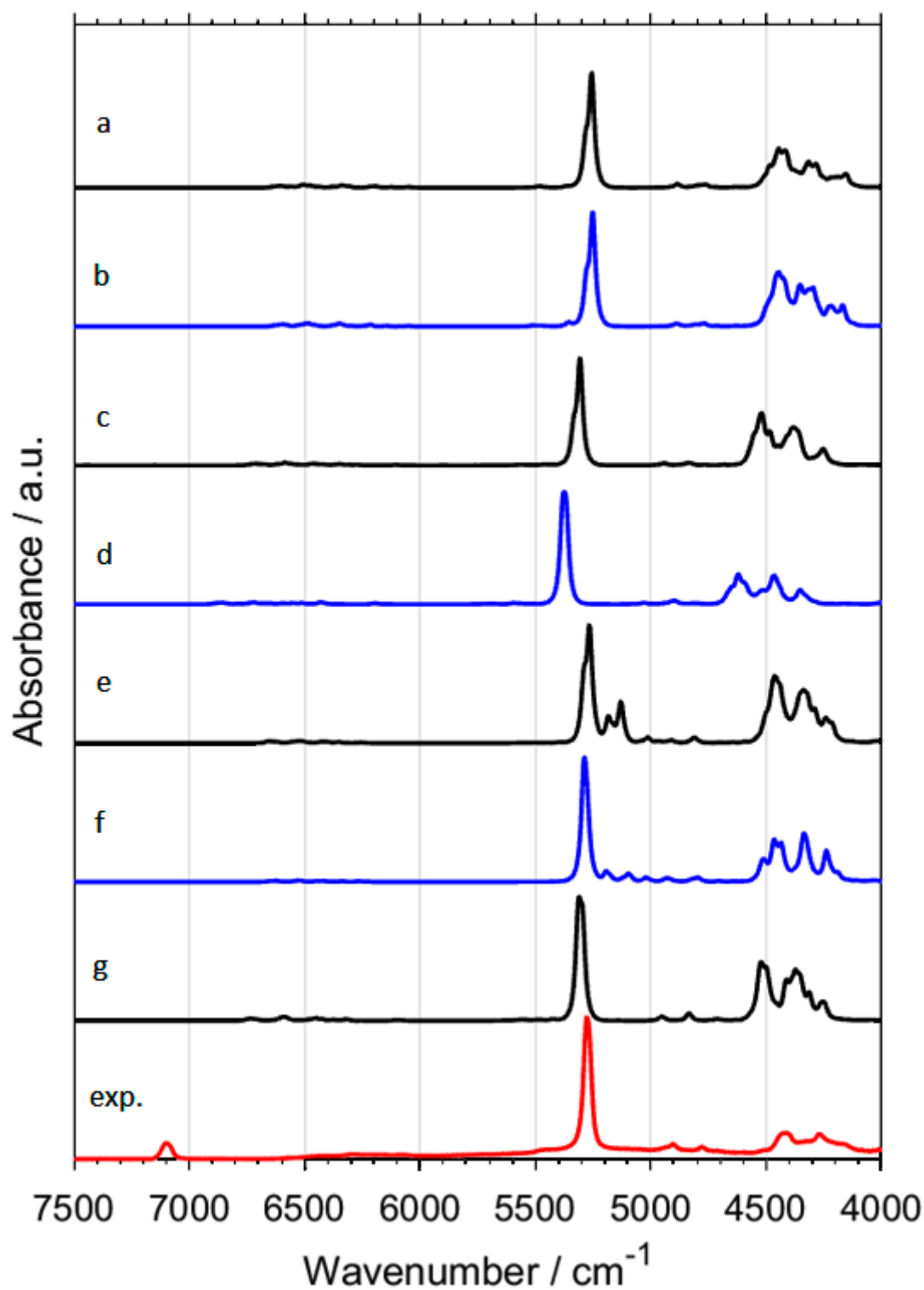


Figure S4. NIR spectra of CD₃CD₂OD calculated with GVPT2 method at different levels of electronic theory; (a) B3LYP-GD3BJ /6-31G(d,p); (b) B3LYP-GD3BJ /6-31G(d,p)//CPCM; (c) B2PLYP-GD3BJ/6-31G(d,p)//CPCM; (d) MP2/6-31G(d,p)//CPCM; (e) B3LYP-GD3BJ/SNST//CPCM; (f) B2PLYP-GD3BJ/def2-TZVP//CPCM; (g) MP2/aug-cc-pVTZ//CPCM. Experimental spectrum (exp.) of CD₃CD₂OD in CCl₄ (0.1 M).

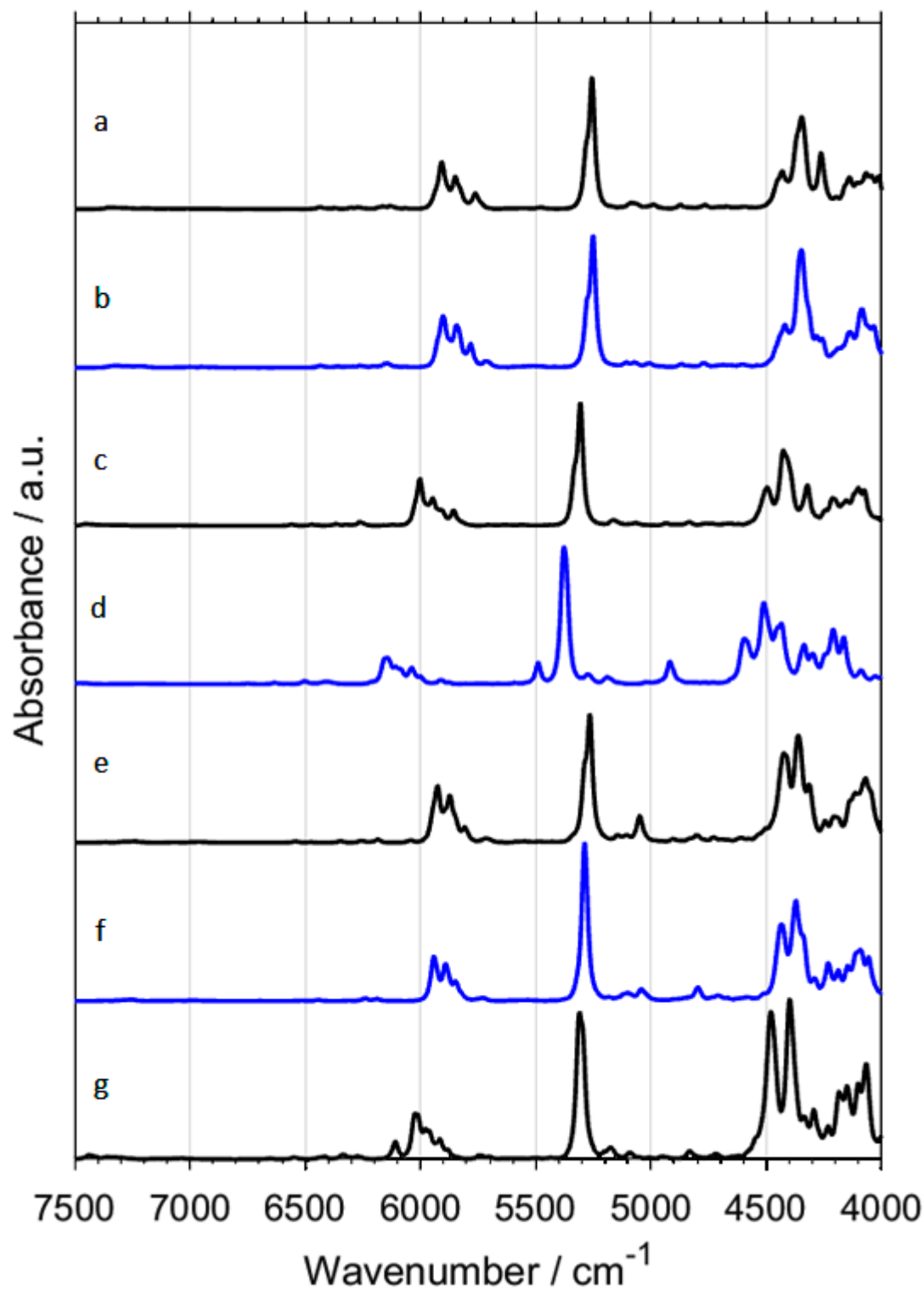


Figure S5. NIR spectra of $\text{CH}_3\text{CD}_2\text{OD}$ calculated with GVPT2 method at different levels of electronic theory; (a) B3LYP-GD3BJ /6-31G(d,p); (b) B3LYP-GD3BJ /6-31G(d,p)//CPCM; (c) B2PLYP-GD3BJ/6-31G(d,p)//CPCM; (d) MP2/6-31G(d,p)//CPCM; (e) B3LYP-GD3BJ/SNST//CPCM; (f) B2PLYP-GD3BJ/def2-TZVP//CPCM; (g) MP2/aug-cc-pVTZ//CPCM.

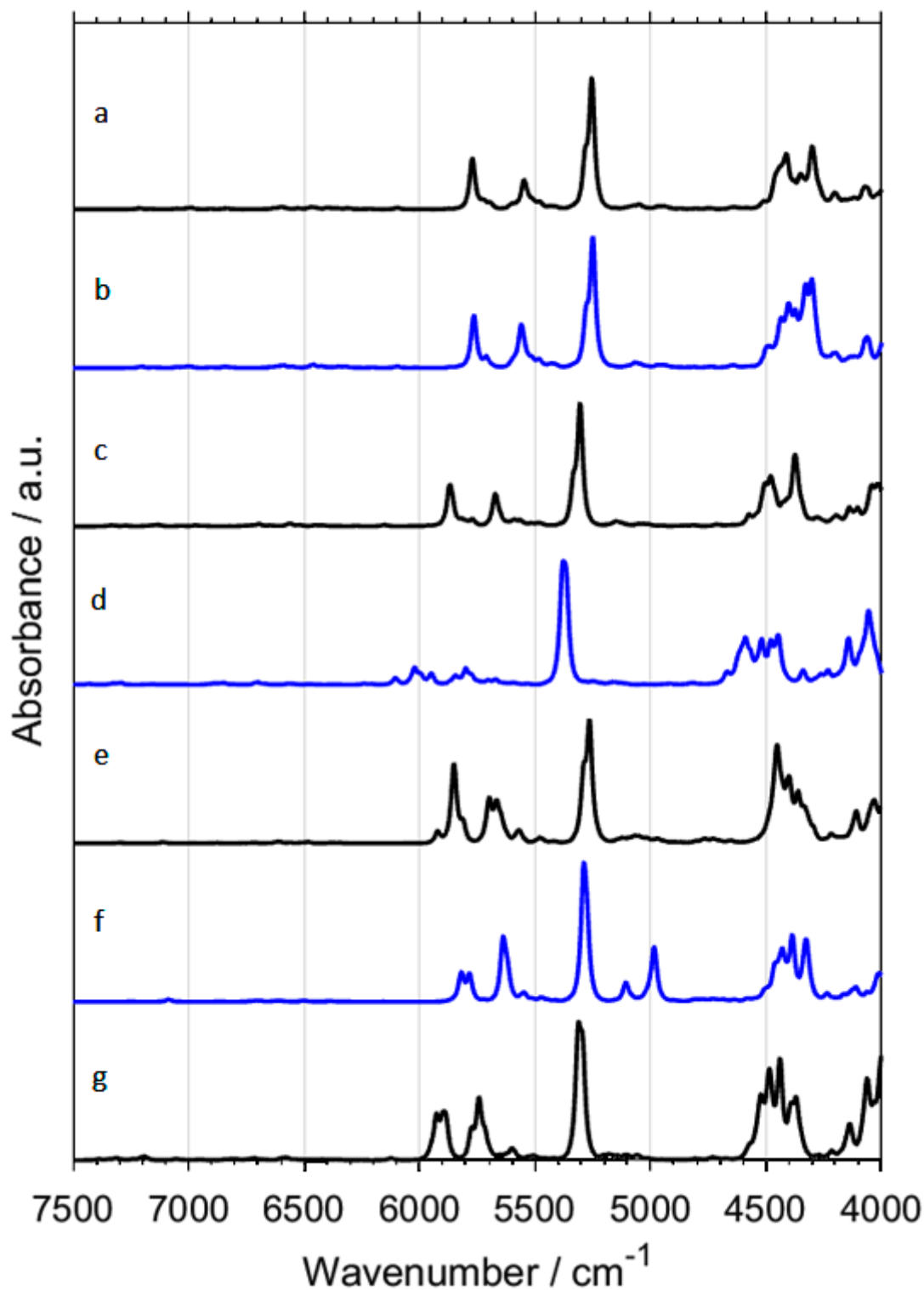


Figure S6. NIR spectra of CD₃CH₂OD calculated with GVPT2 method at different levels of electronic theory; (a) B3LYP-GD3BJ /6-31G(d,p); (b) B3LYP-GD3BJ /6-31G(d,p)//CPCM; (c) B2PLYP-GD3BJ/6-31G(d,p)//CPCM; (d) MP2/6-31G(d,p)//CPCM; (e) B3LYP-GD3BJ/SNST//CPCM; (f) B2PLYP-GD3BJ/def2-TZVP//CPCM; (g) MP2/aug-cc-pVTZ//CPCM.

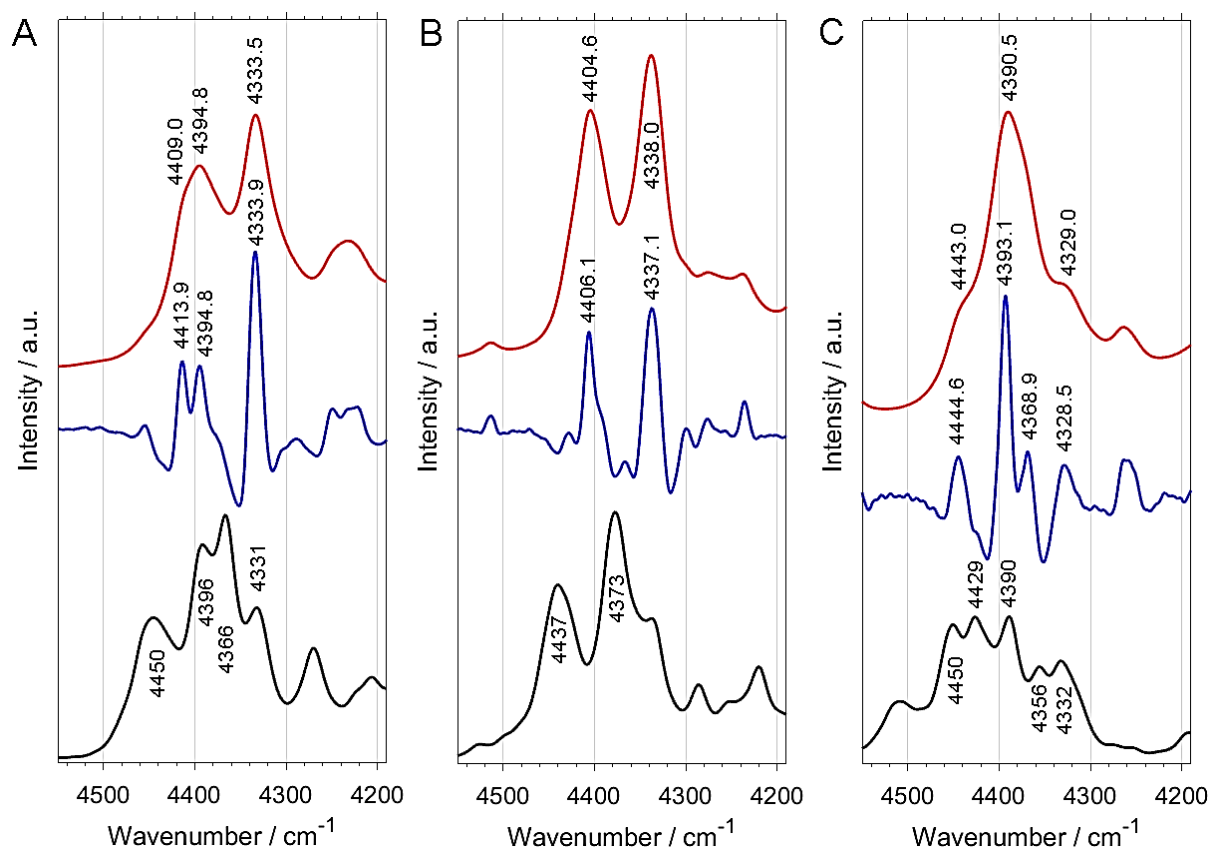


Figure S7. The details of NIR spectra of (A) $\text{CH}_3\text{CH}_2\text{OH}$; (B) $\text{CH}_3\text{CD}_2\text{OH}$; (C) $\text{CD}_3\text{CH}_2\text{OH}$ in the 4550-4200 cm^{-1} . From up to bottom: experimental NIR spectrum (red line); second derivative spectrum, multiplied by -1 (blue line); theoretical (B2PLYP-GD3BJ/def2-TZVP//CPCM) spectrum (black line).

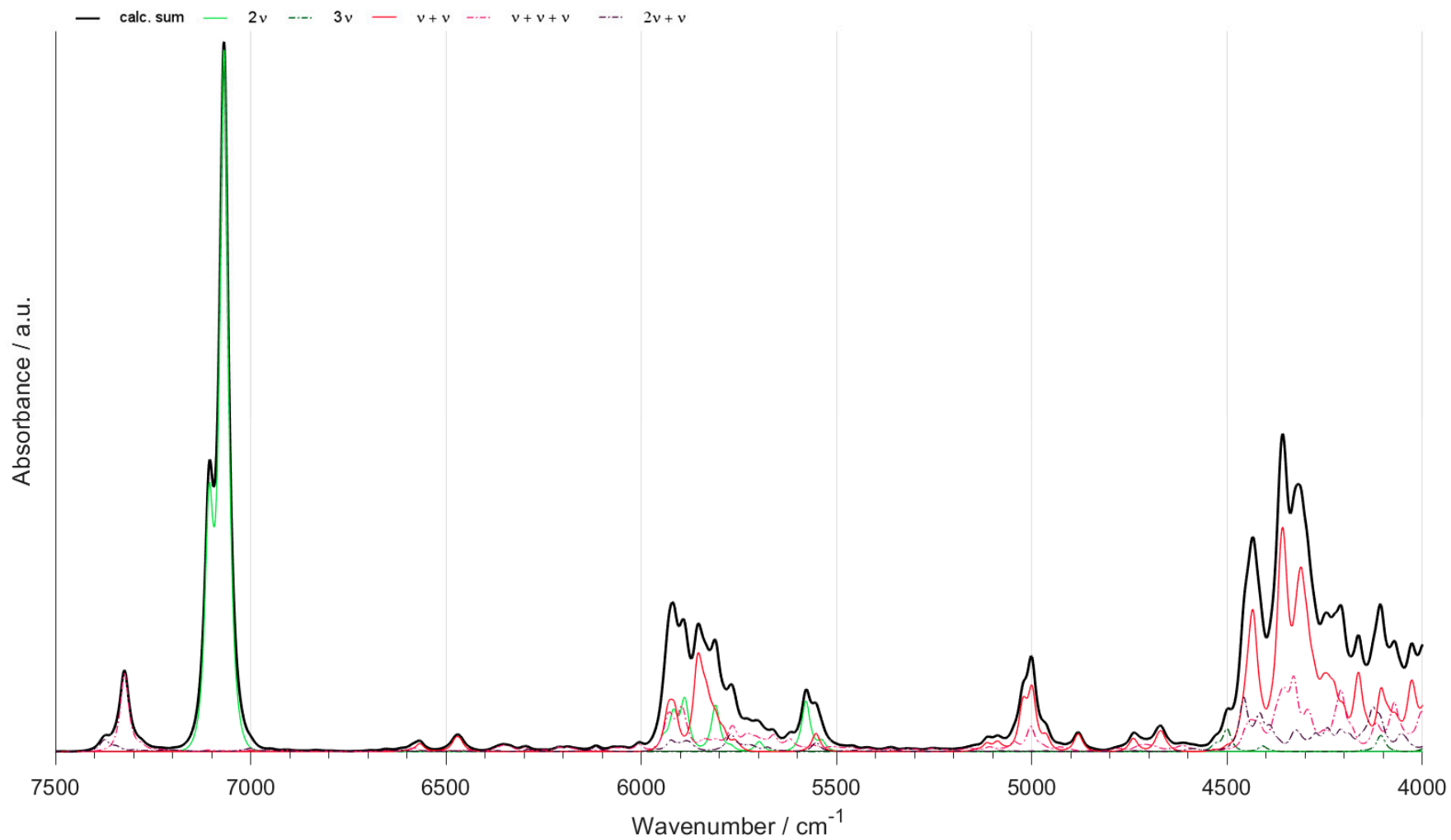


Figure S8. (Enlarged) NIR spectra of $\text{CH}_3\text{CH}_2\text{OH}$ calculated with GVPT2 method at B3LYP-GD3BJ/6-31G(d,p) level of electronic theory

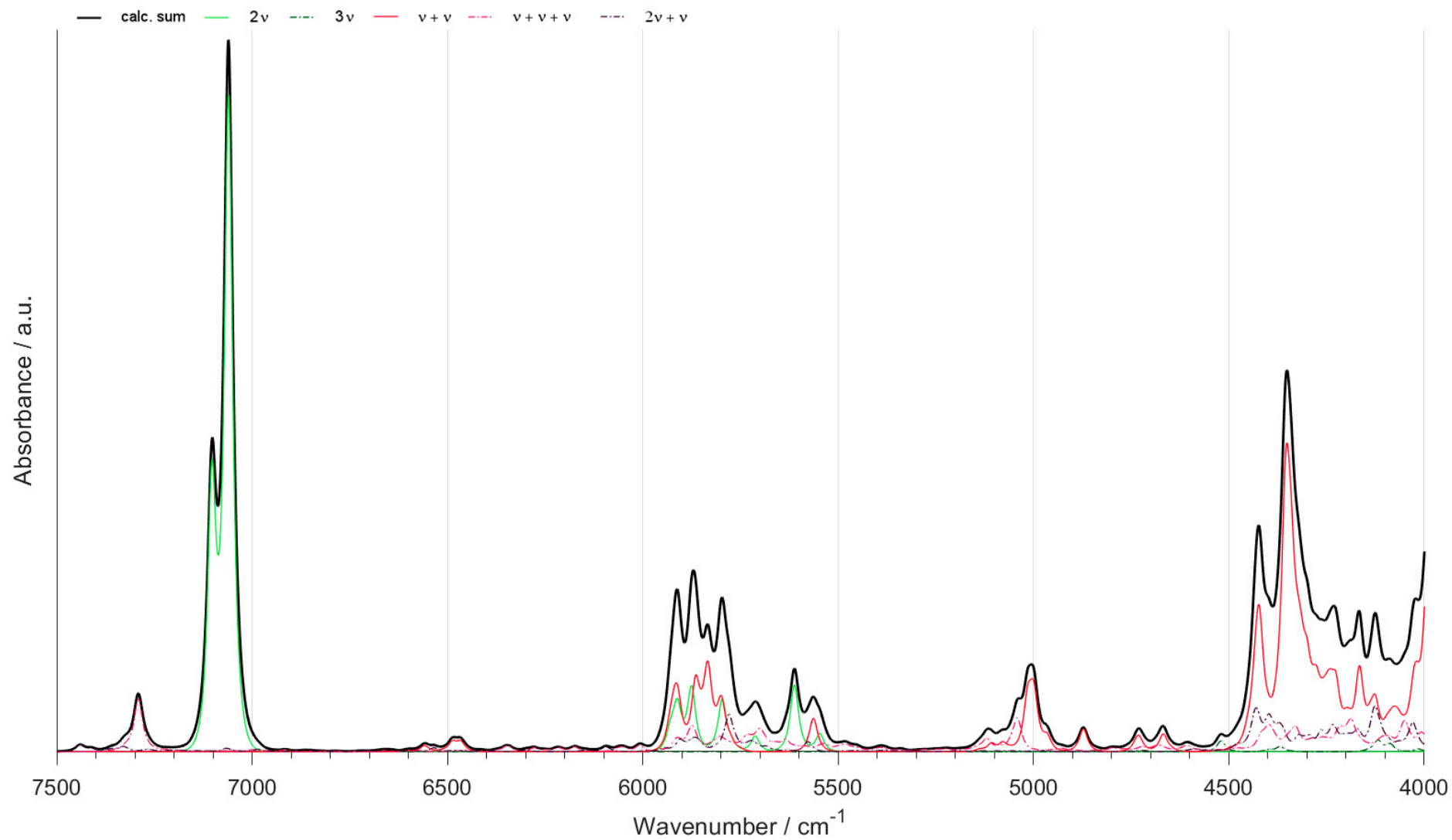


Figure S9. (High-resolution copy of Figure 1) NIR spectra of $\text{CH}_3\text{CH}_2\text{OH}$ calculated with GVPT2 method at B3LYP-GD3BJ/6-31G(d,p)//CPCM level of electronic theory.

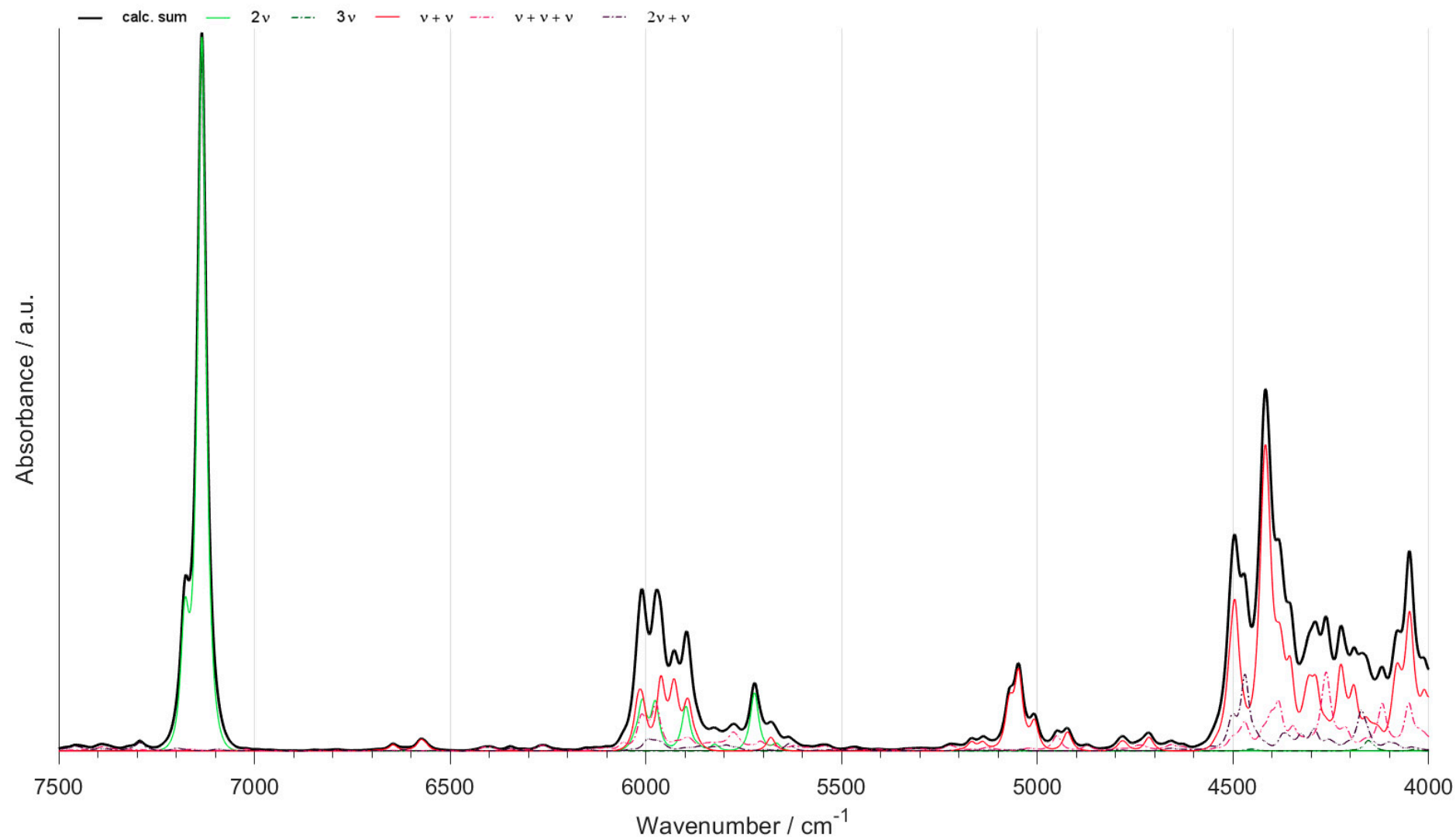
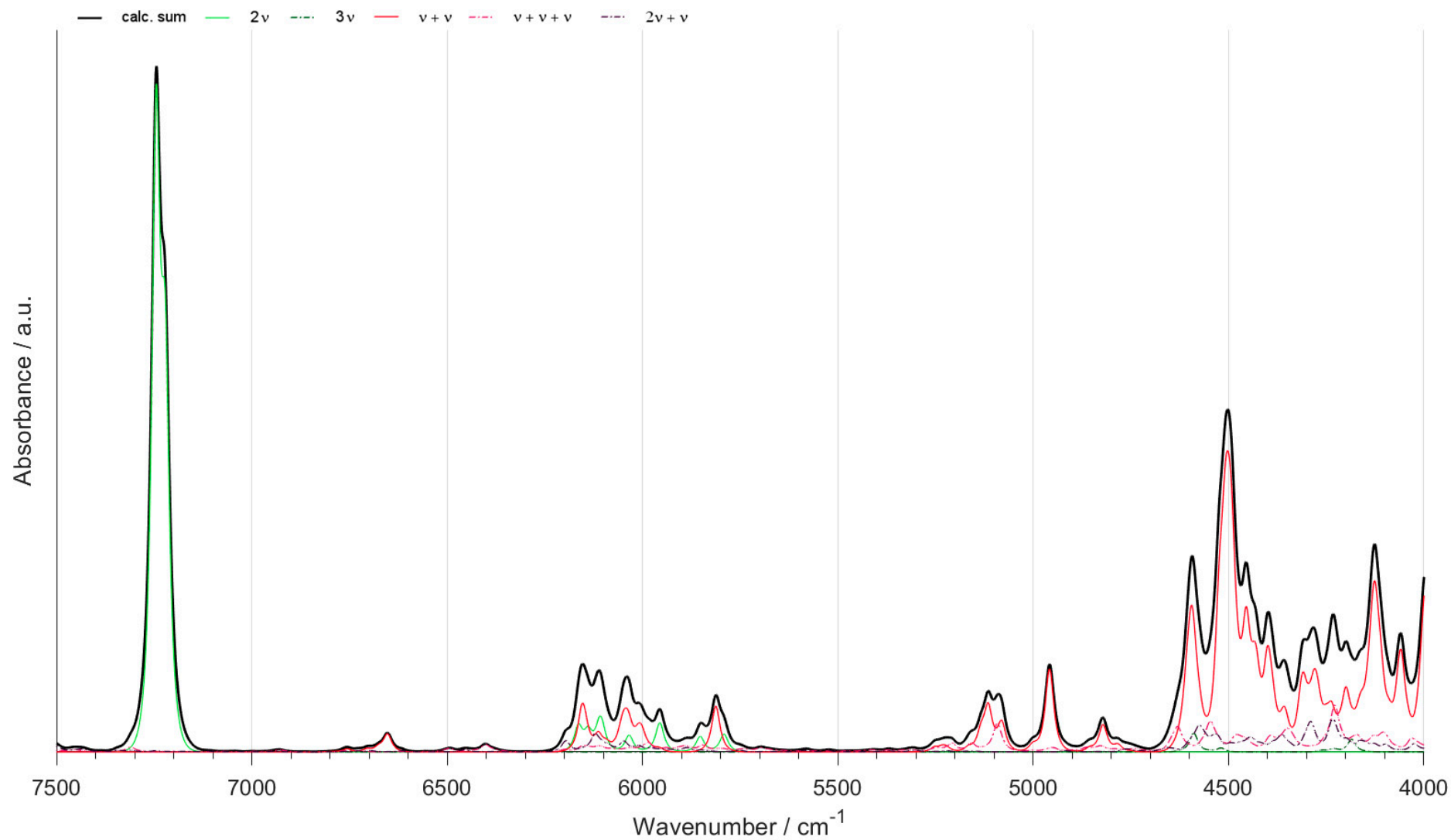


Figure S10. (High-resolution copy of Figure 1) NIR spectra of $\text{CH}_3\text{CH}_2\text{OH}$ calculated with GVPT2 method at B2PLYP-GD3BJ/6-31G(d,p)//CPCM level of electronic theory.



#

Figure S11. (High-resolution copy of Figure 1) NIR spectra of $\text{CH}_3\text{CH}_2\text{OH}$ calculated with GVPT2 method at MP2/6-31G(d,p)//CPCM level of electronic theory.

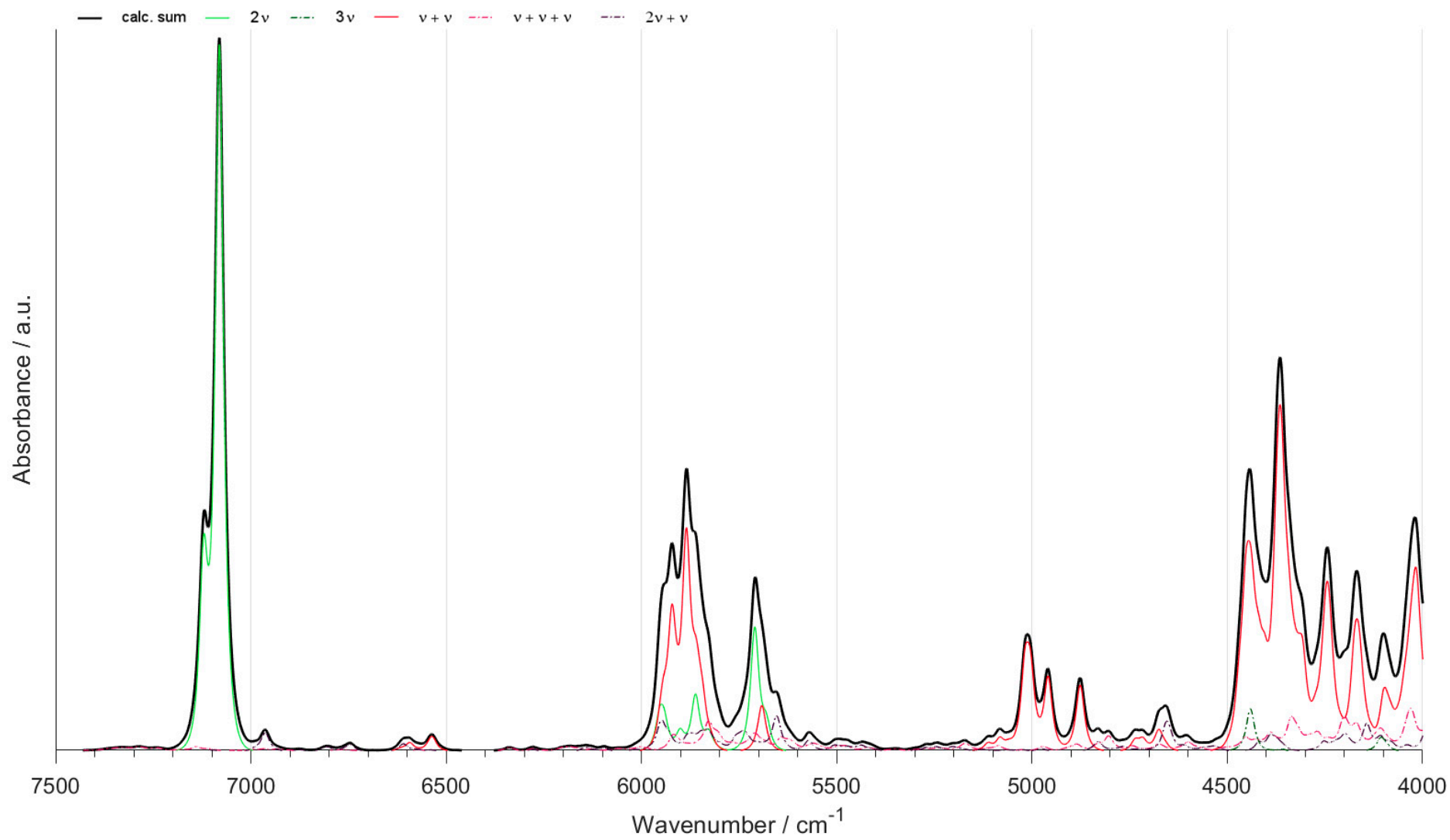


Figure S12. (High-resolution copy of Figure 1) NIR spectra of $\text{CH}_3\text{CH}_2\text{OH}$ calculated with GVPT2 method at B3LYP-GD3BJ/SNST//CPCM level of electronic theory.

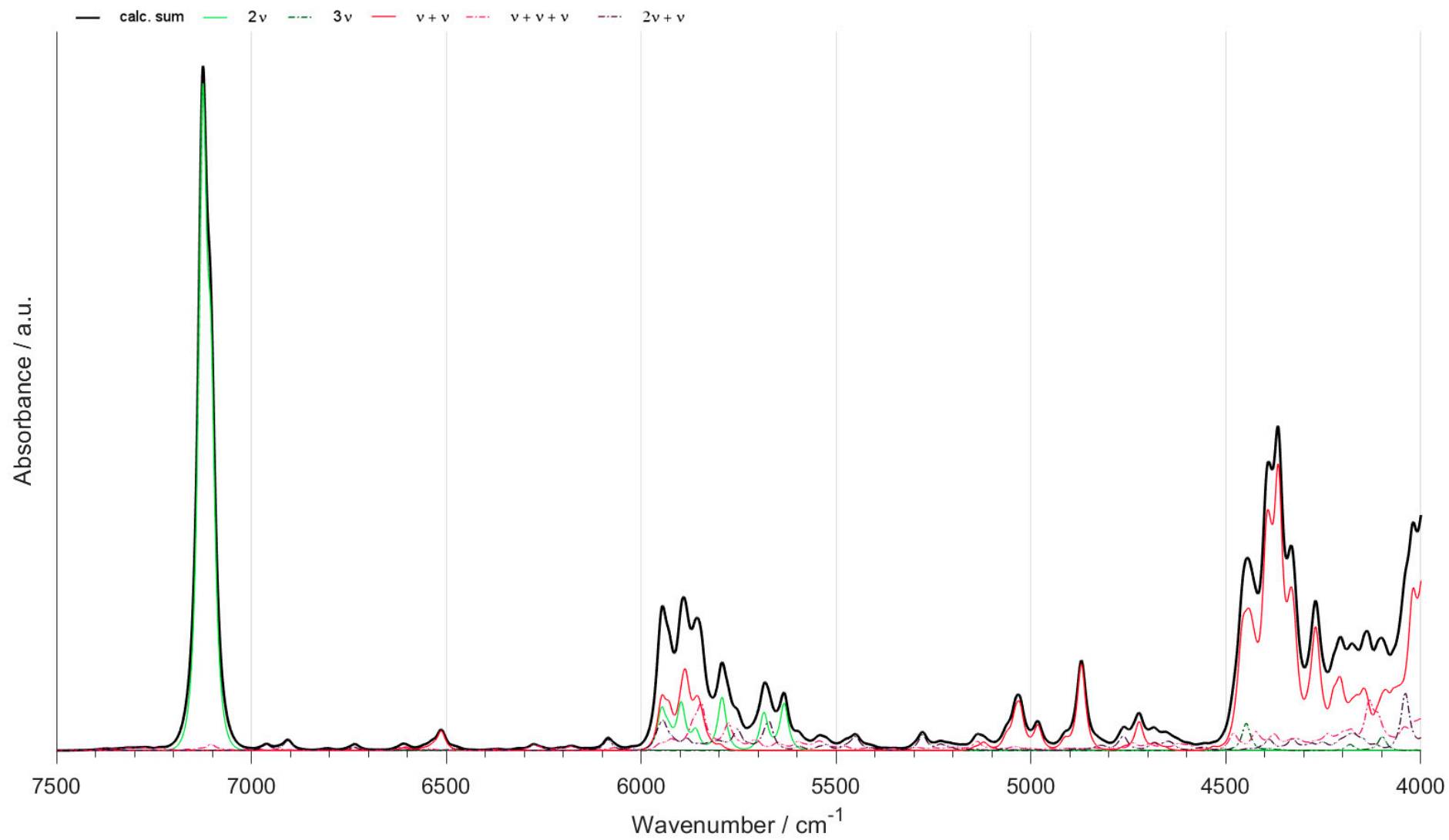


Figure S13. (High-resolution copy of Figure 1) NIR spectra of $\text{CH}_3\text{CH}_2\text{OH}$ calculated with GVPT2 method at B2PLYP-GD3BJ/def2-TZVP//CPCM level of electronic theory.

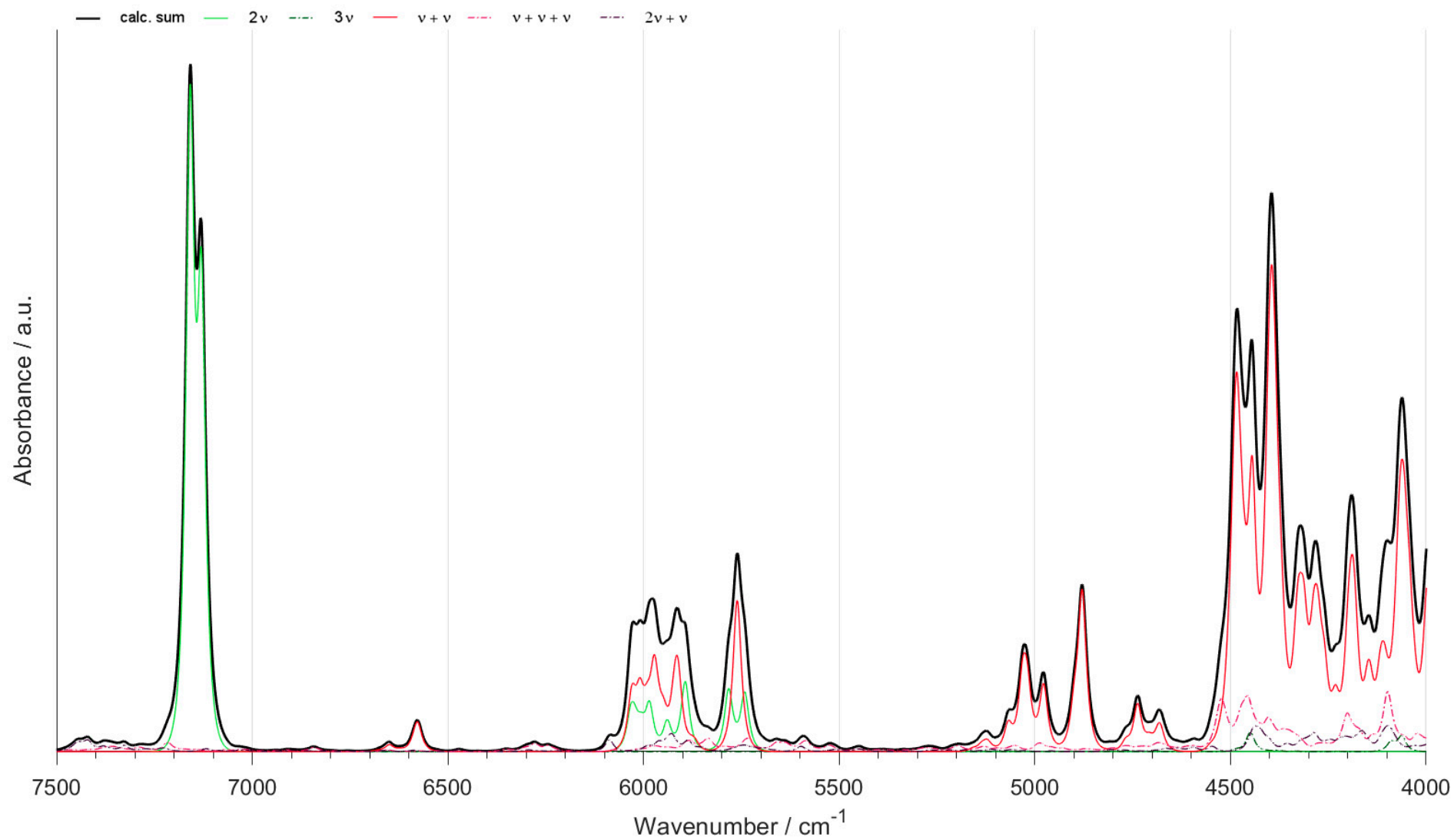


Figure S14. (High-resolution copy of Figure 1) NIR spectra of $\text{CH}_3\text{CH}_2\text{OH}$ calculated with GVPT2 method at MP2/aug-cc-pVTZ//CPCM level of electronic theory.

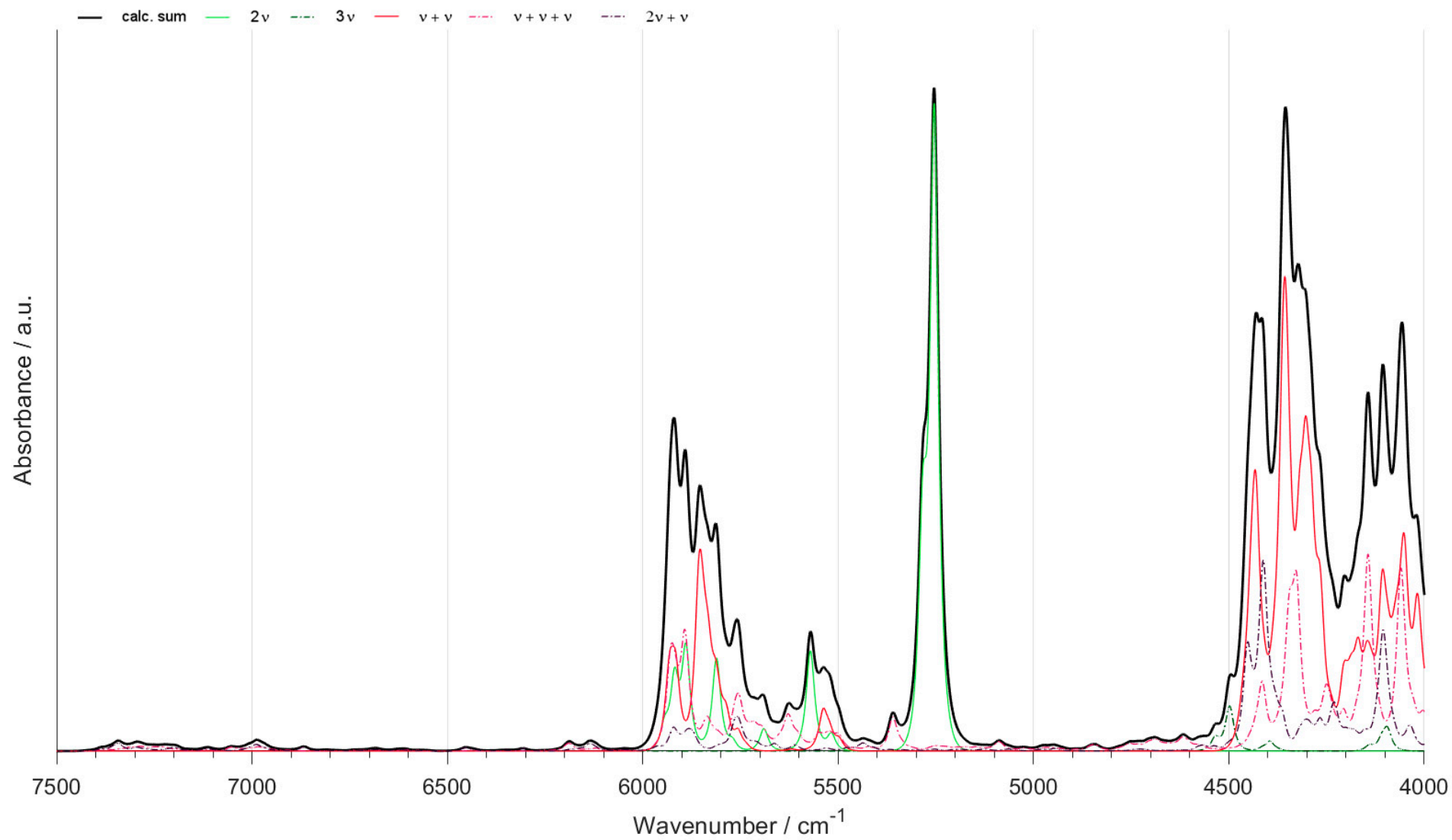


Figure S15. (High-resolution copy of Figure 2) NIR spectra of $\text{CH}_3\text{CH}_2\text{OD}$ calculated with GVPT2 method at B3LYP-GD3BJ/6-31G(d,p) level of electronic theory.

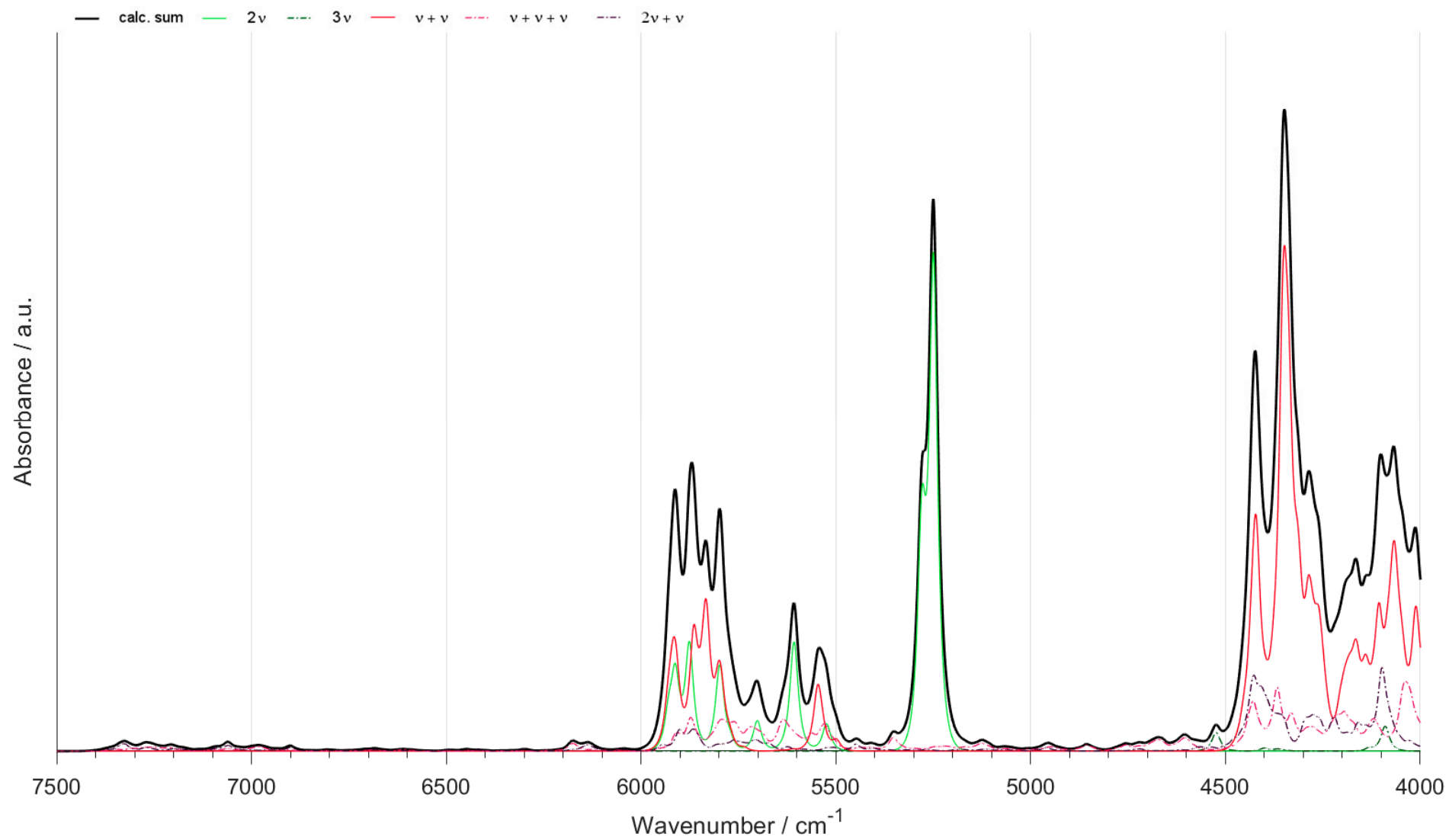


Figure S16. (High-resolution copy of Figure 2) NIR spectra of $\text{CH}_3\text{CH}_2\text{OD}$ calculated with GVPT2 method at B3LYP-GD3BJ/6-31G(d,p)//CPCM level of electronic theory.

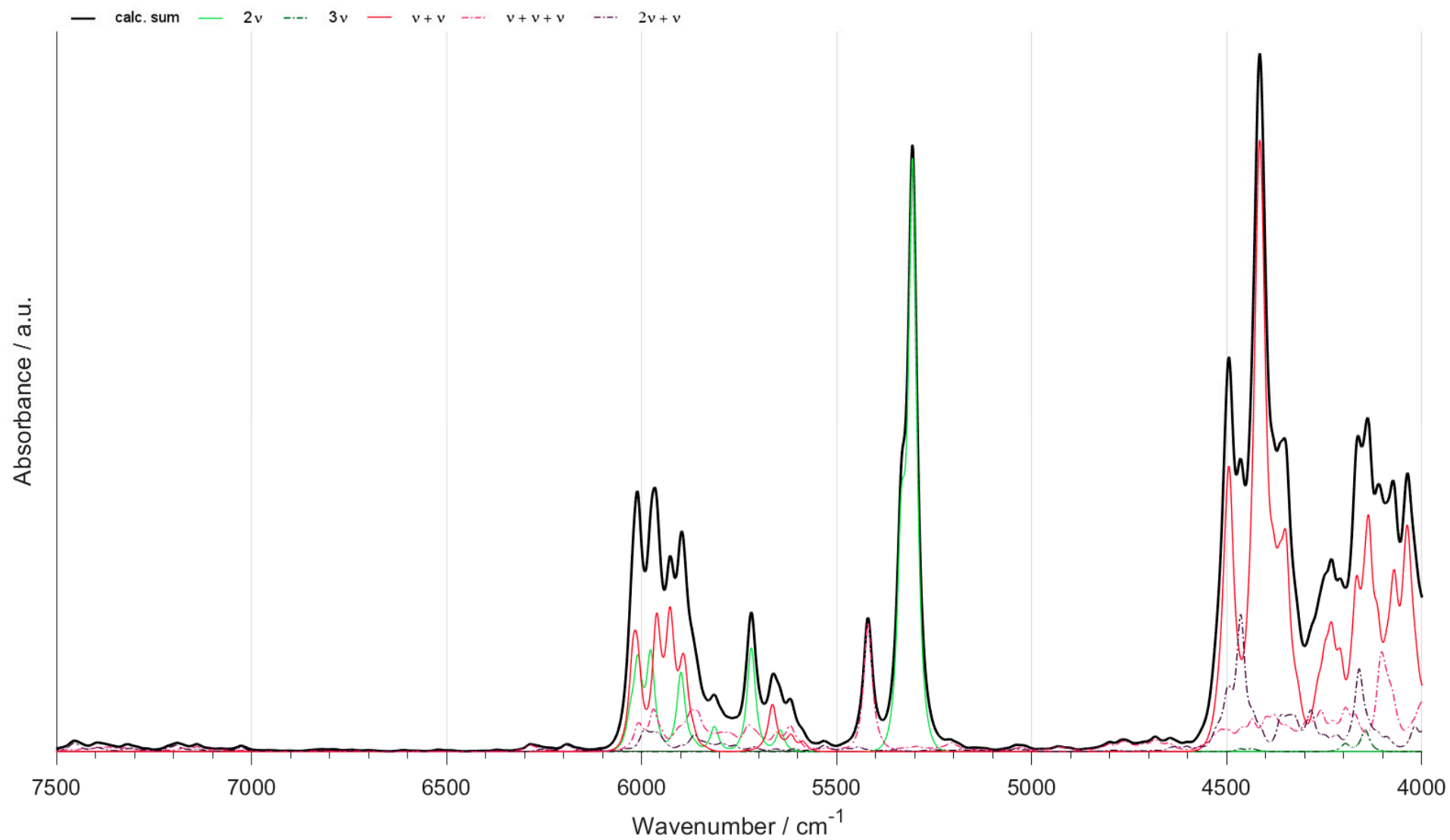


Figure S17. (High-resolution copy of Figure 2) NIR spectra of $\text{CH}_3\text{CH}_2\text{OD}$ calculated with GVPT2 method at B2PLYP-GD3BJ/6-31G(d,p)//CPCM level of electronic theory.

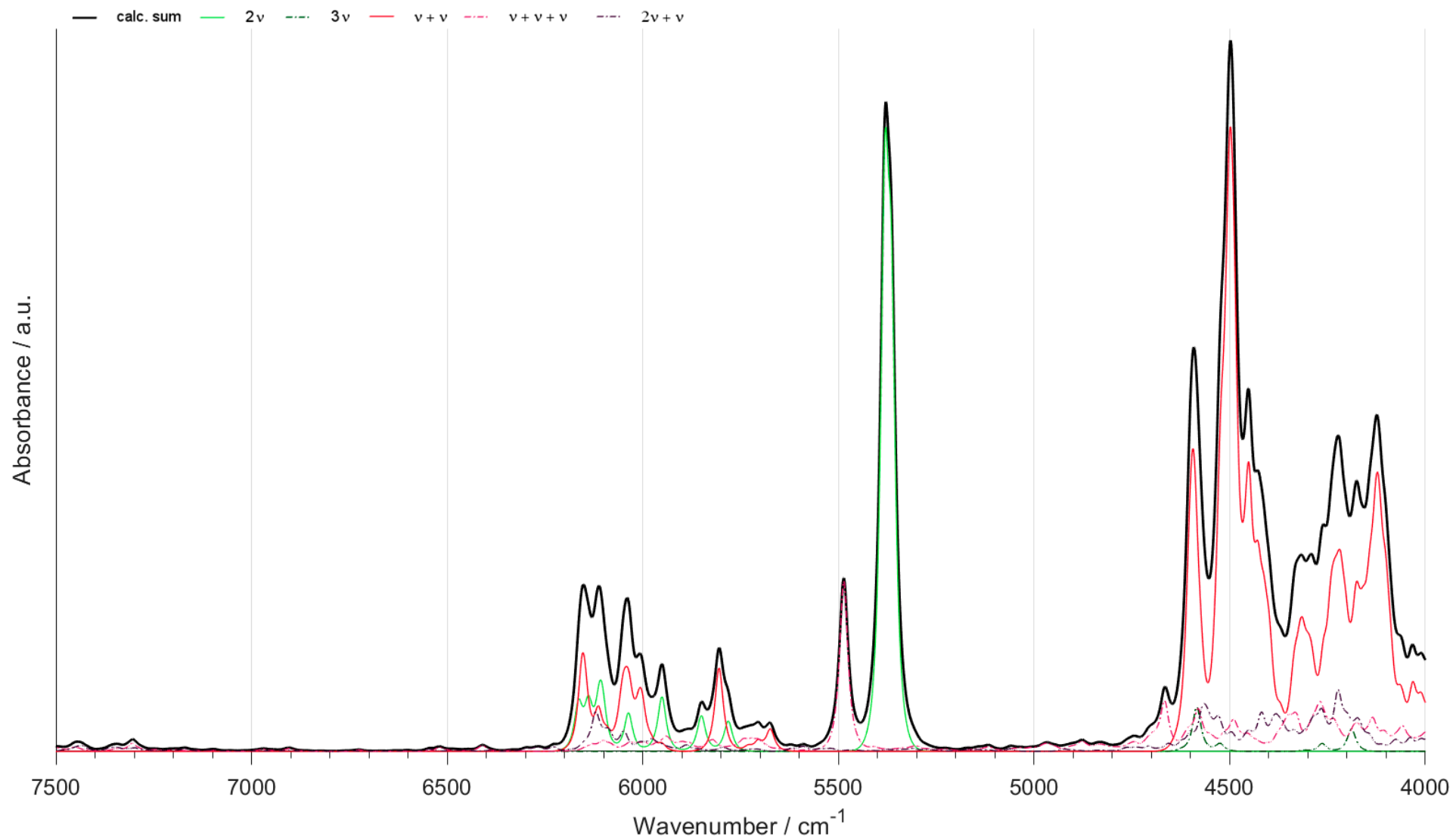


Figure S18. (High-resolution copy of Figure 2) NIR spectra of $\text{CH}_3\text{CH}_2\text{OD}$ calculated with GVPT2 method at MP2/6-31G(d,p)//CPCM t level of electronic theory.

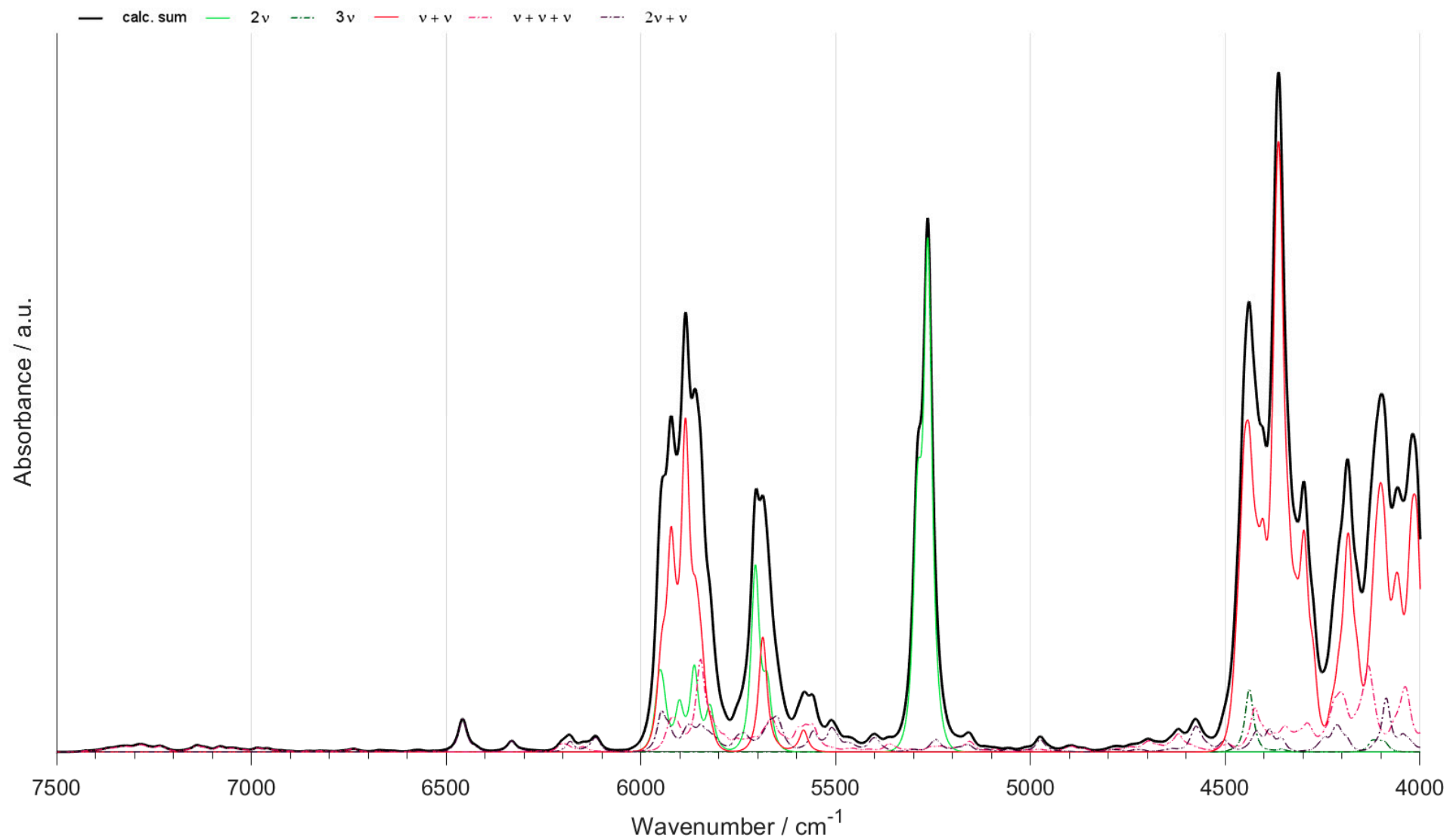


Figure S19. (High-resolution copy of Figure 2) NIR spectra of $\text{CH}_3\text{CH}_2\text{OD}$ calculated with GVPT2 method at B3LYP-GD3BJ/SNST//CPCM level of electronic theory.

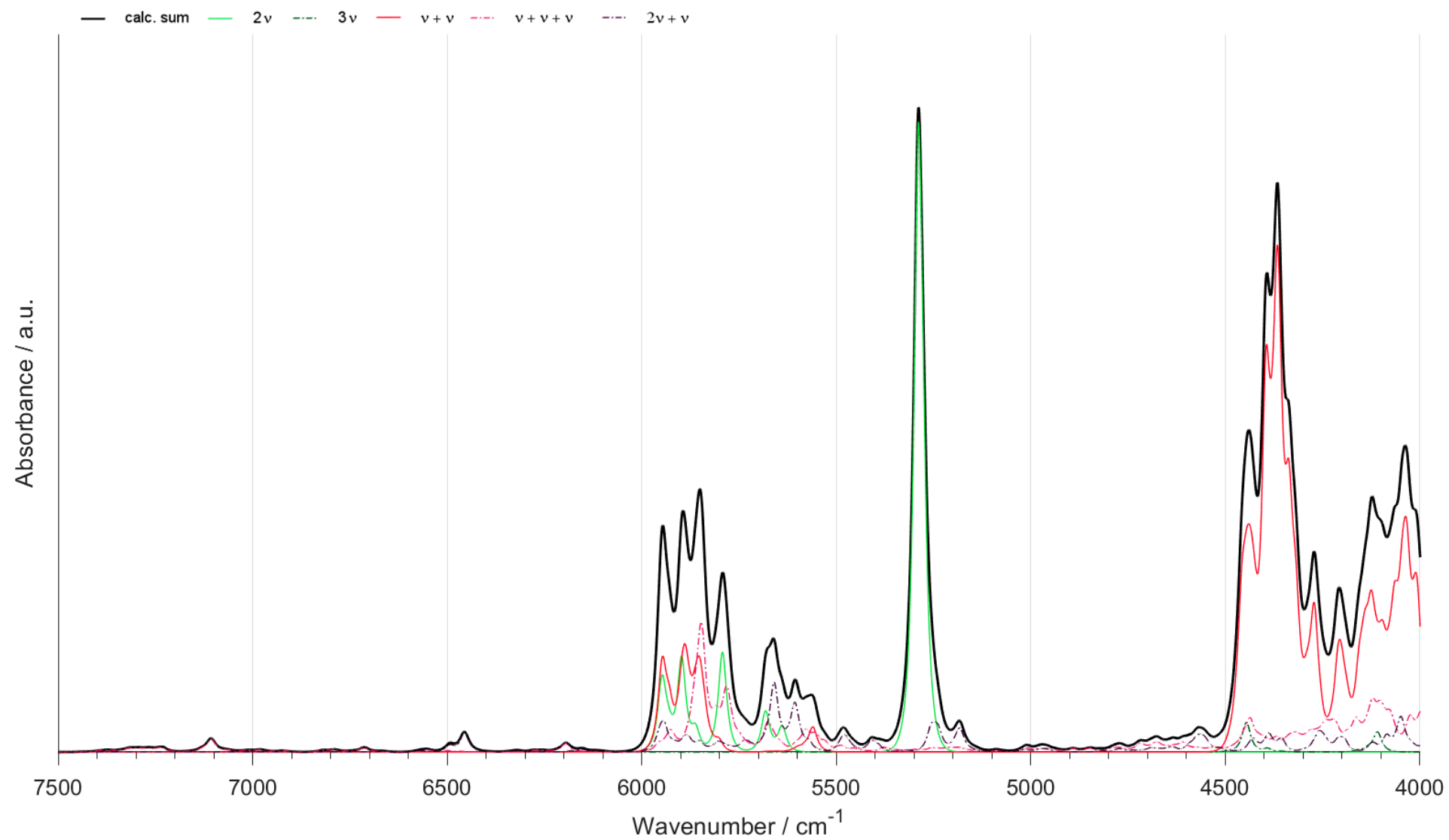


Figure S20. (High-resolution copy of Figure 2) NIR spectra of $\text{CH}_3\text{CH}_2\text{OD}$ calculated with GVPT2 method at B2PLYP-GD3BJ/def2-TZVP//CPCM level of electronic theory.

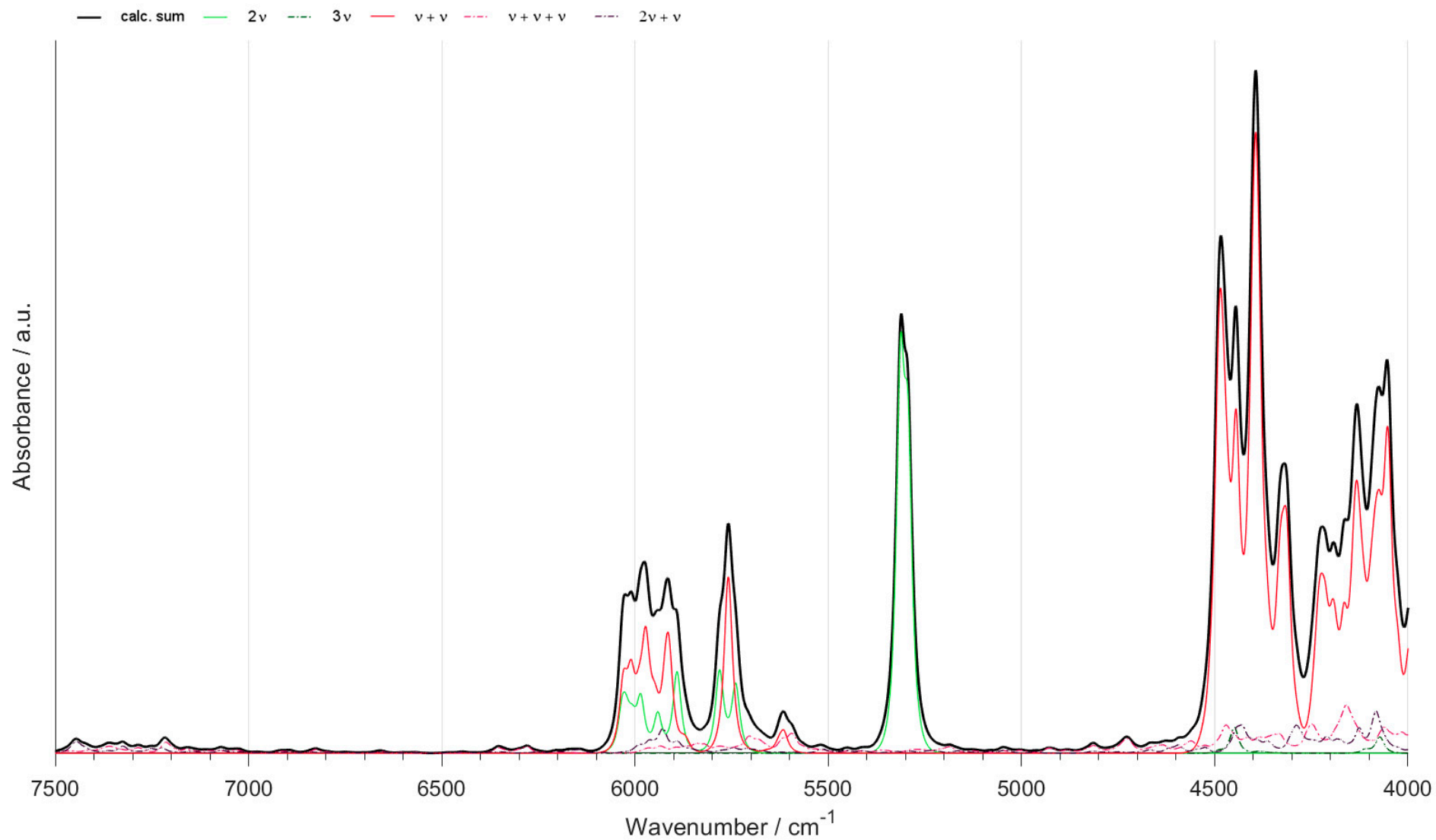


Figure S21. (High-resolution copy of Figure 2) NIR spectra of $\text{CH}_3\text{CH}_2\text{OD}$ calculated with GVPT2 method at MP2/aug-cc-pVTZ//CPCM level of electronic theory.

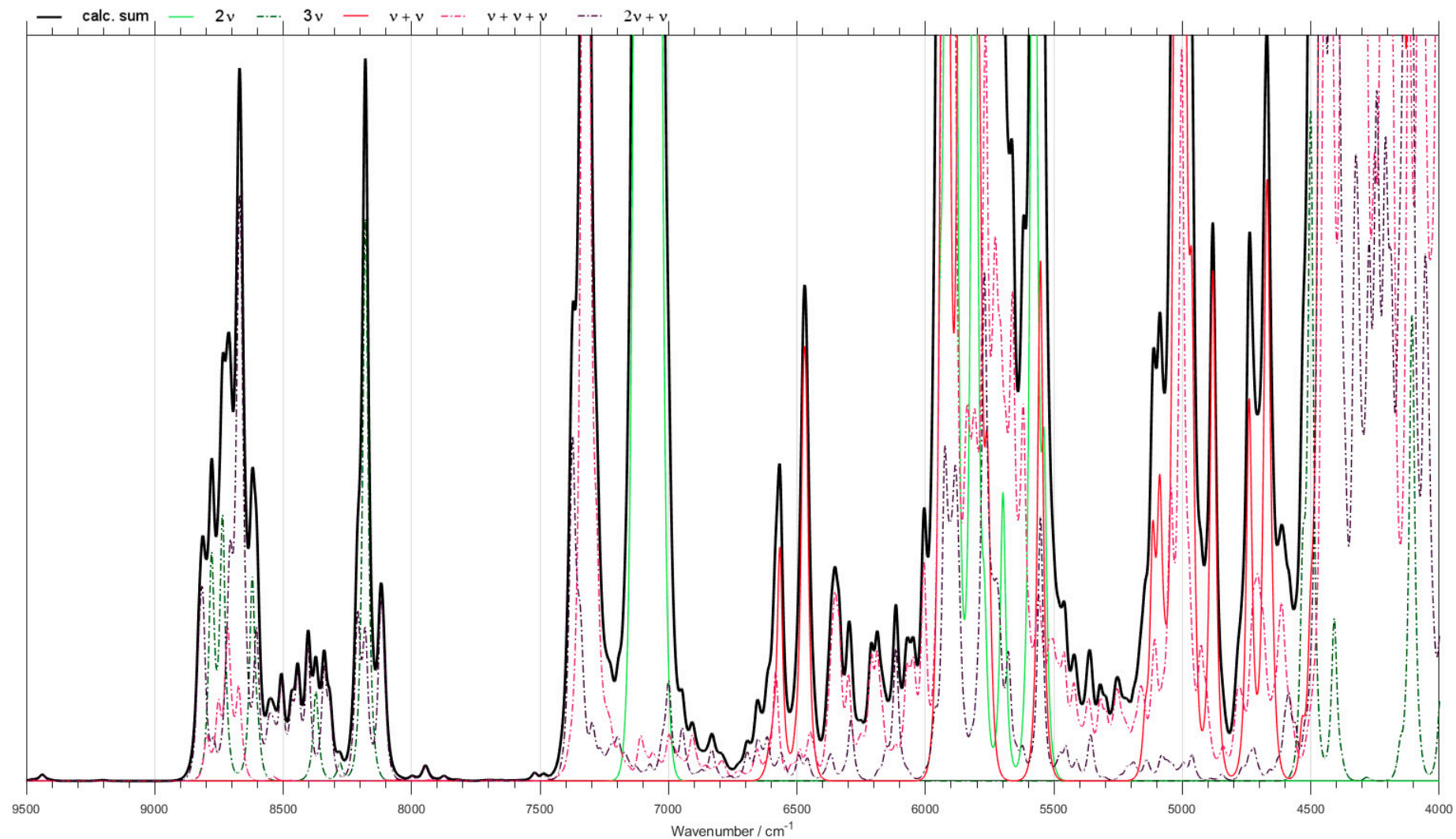


Figure S22. (High-resolution copy of Figure 3) Contributions from minor bands in NIR spectra of $\text{CH}_3\text{CH}_2\text{OH}$ calculated with GVPT2 method at B3LYP-GD3BJ /6-31G(d,p) level of electronic theory.

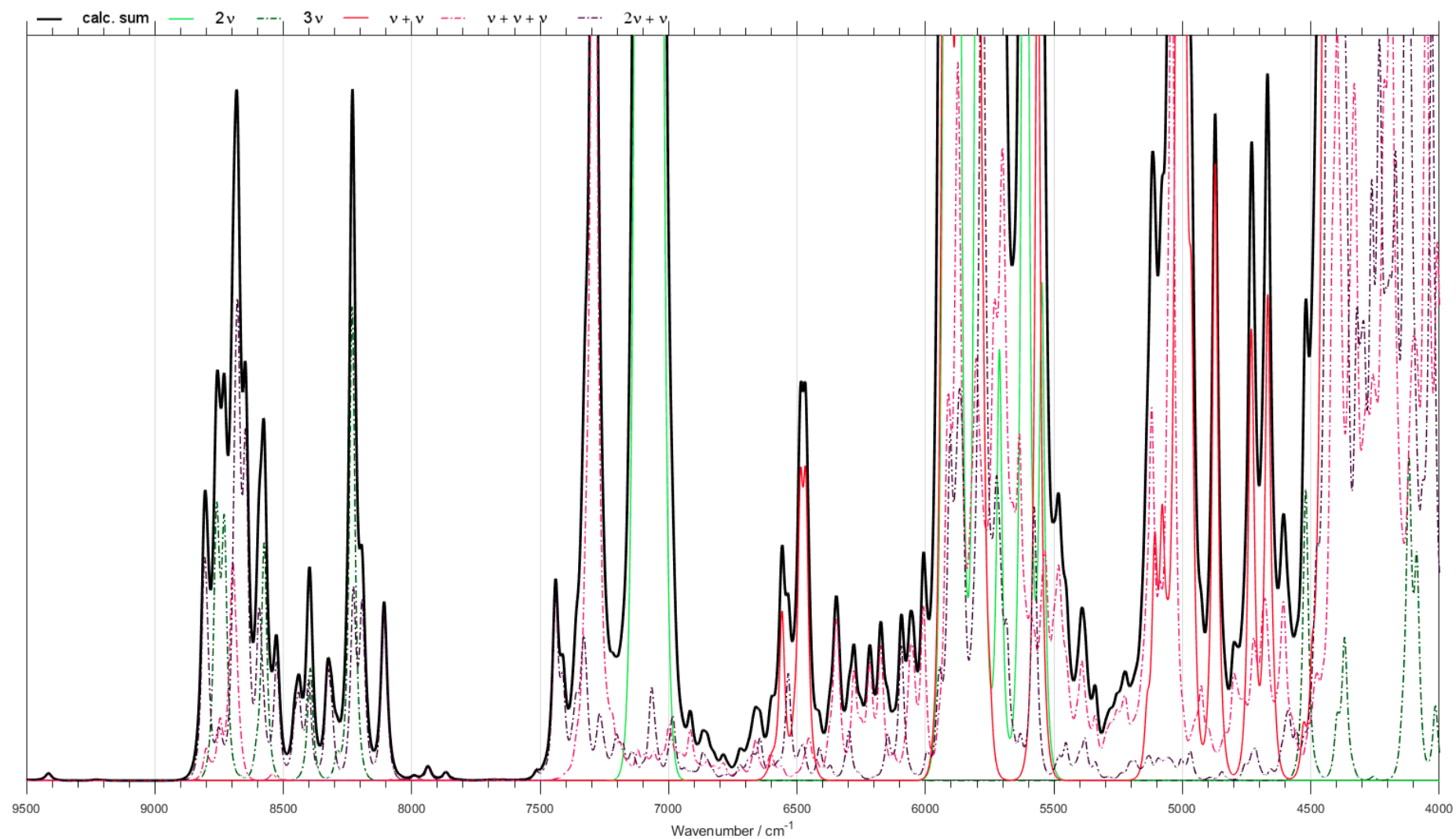


Figure S23. (High-resolution copy of Figure 3) Contributions from minor bands in NIR spectra of $\text{CH}_3\text{CH}_2\text{OH}$ calculated with GVPT2 method at B3LYP-GD3BJ/6-31G(d,p)//CPCM level of electronic theory.

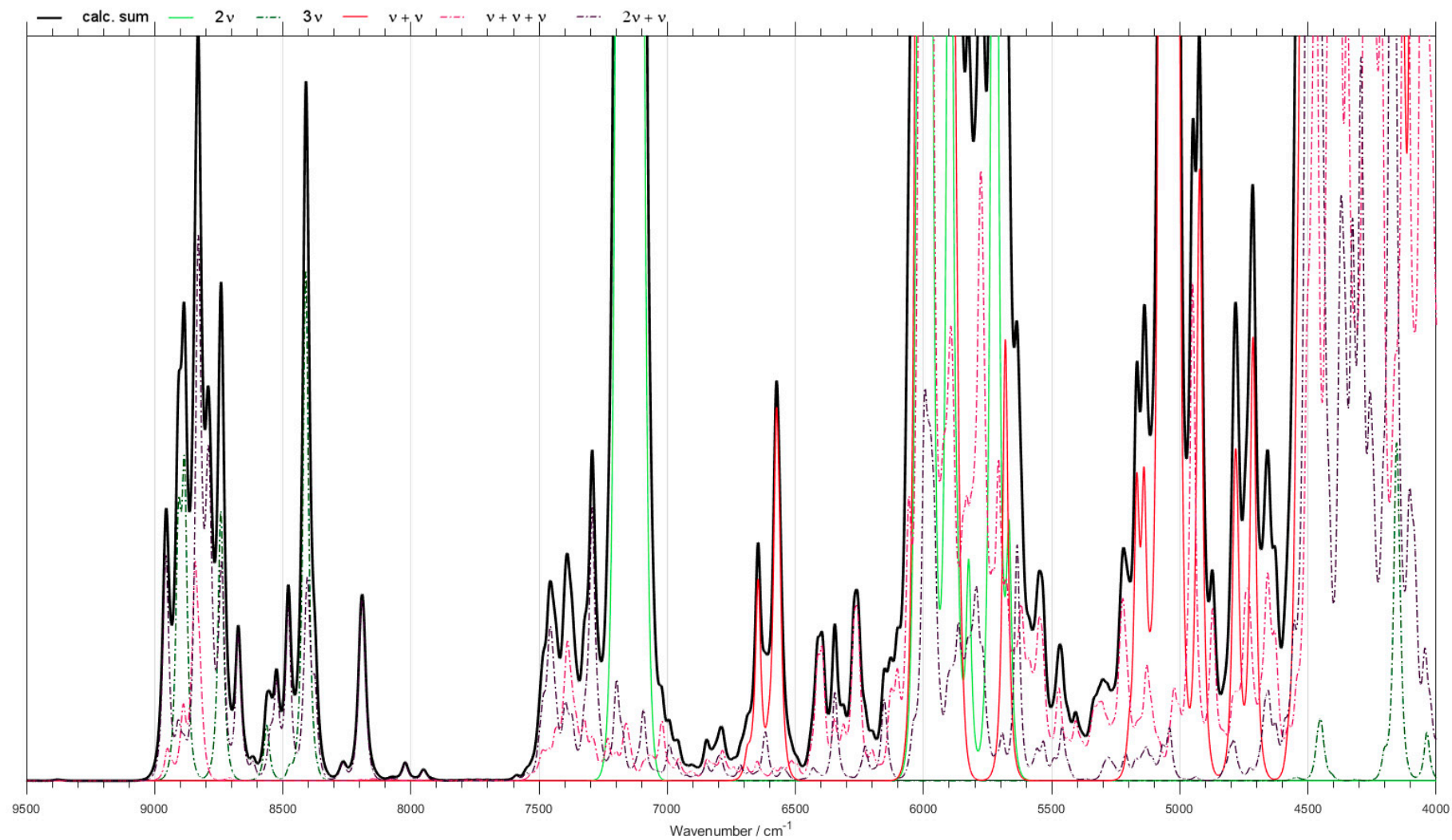


Figure S24. (High-resolution copy of Figure 3) Contributions from minor bands in NIR spectra of $\text{CH}_3\text{CH}_2\text{OH}$ calculated with GVPT2 method at B2PLYP-GD3BJ/6-31G(d,p)//CPCM level of electronic theory.

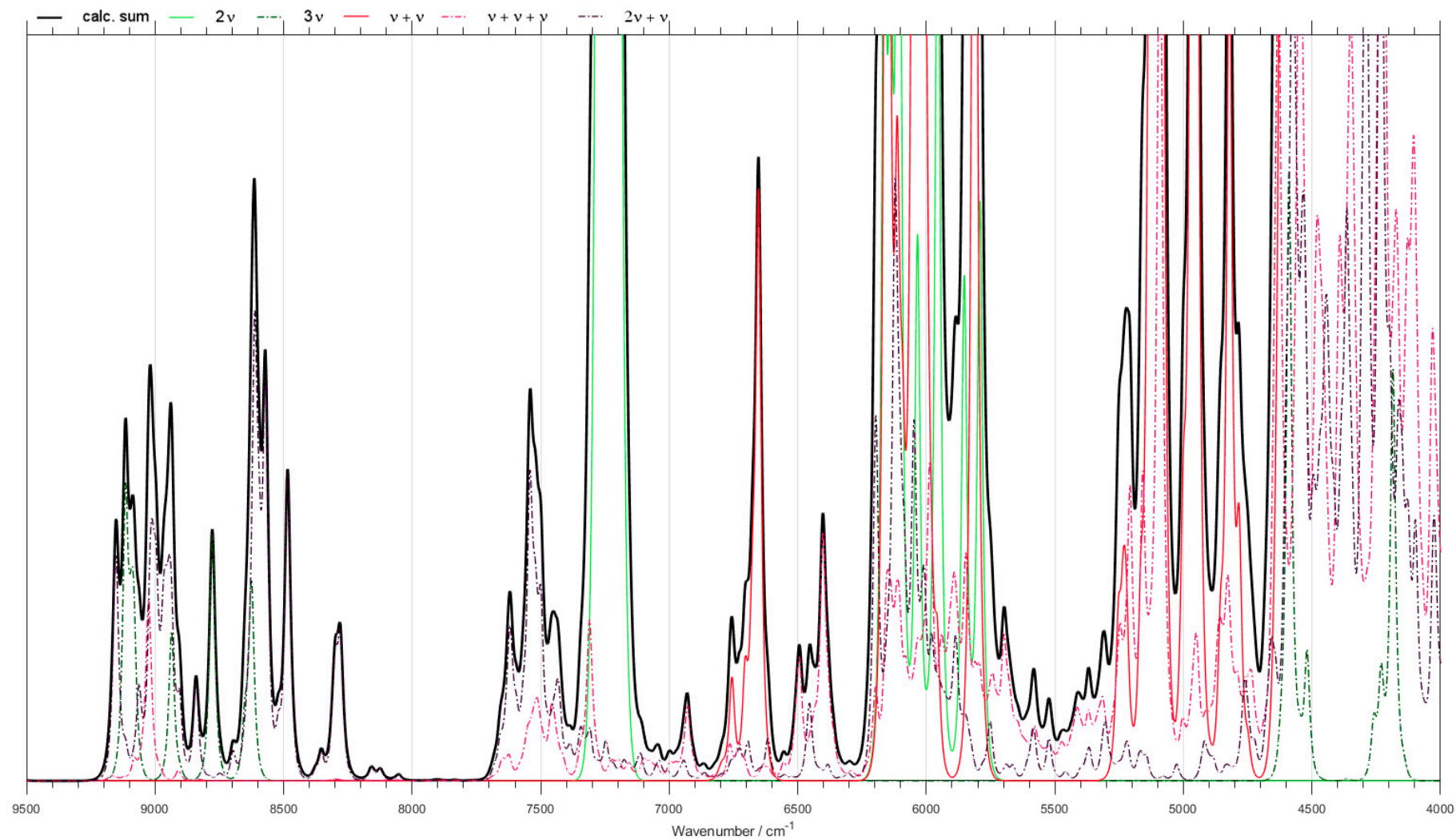


Figure S25. (High-resolution copy of Figure 2) Contributions from minor bands in NIR spectra of $\text{CH}_3\text{CH}_2\text{OH}$ calculated with GVPT2 method at MP2/6-31G(d,p)//CPCM level of electronic theory.

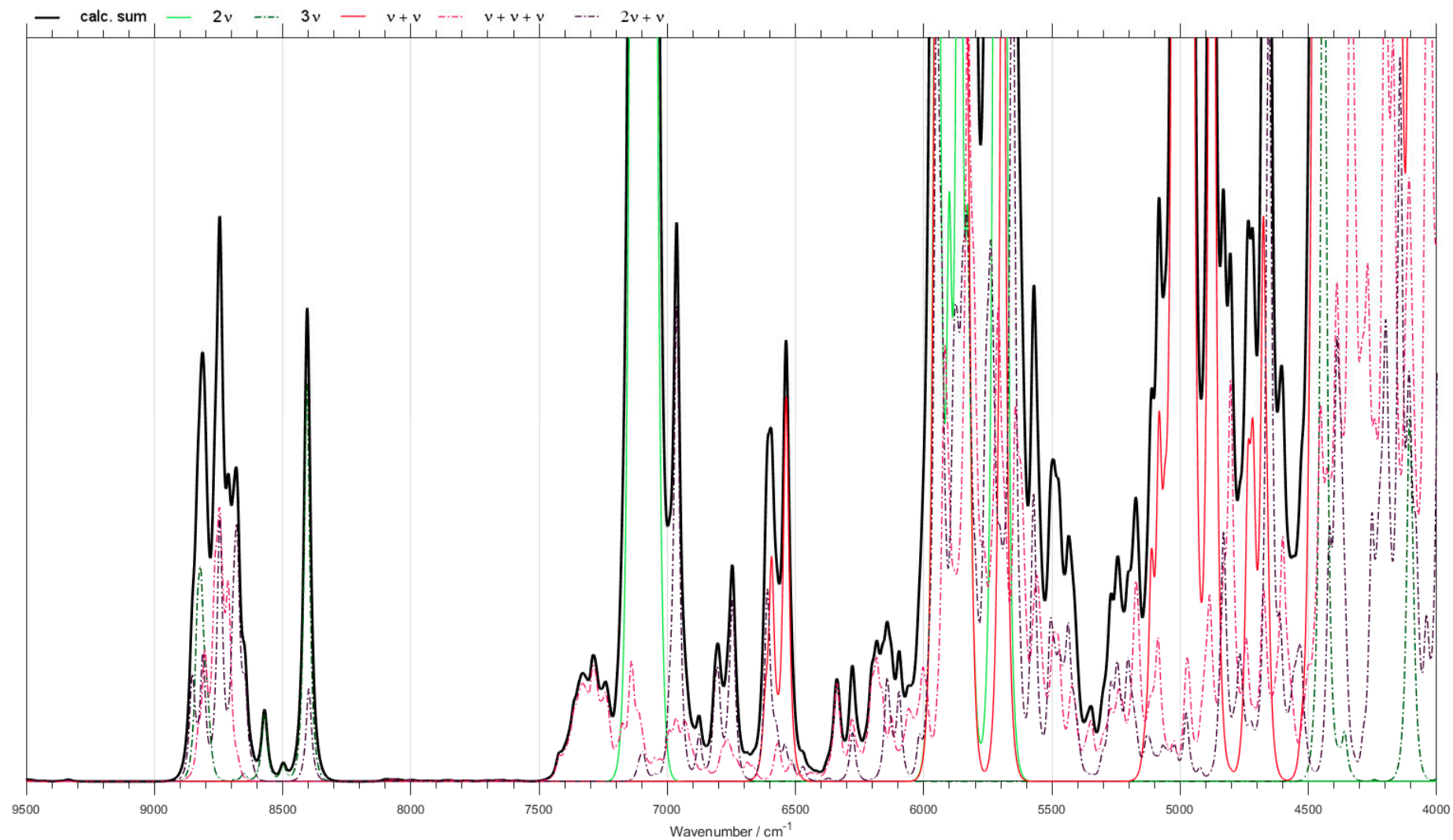


Figure S26. (High-resolution copy of Figure 3) Contributions from minor bands in NIR spectra of $\text{CH}_3\text{CH}_2\text{OH}$ calculated with GVPT2 method at B3LYP-GD3BJ/SNST//CPCM level of electronic theory.

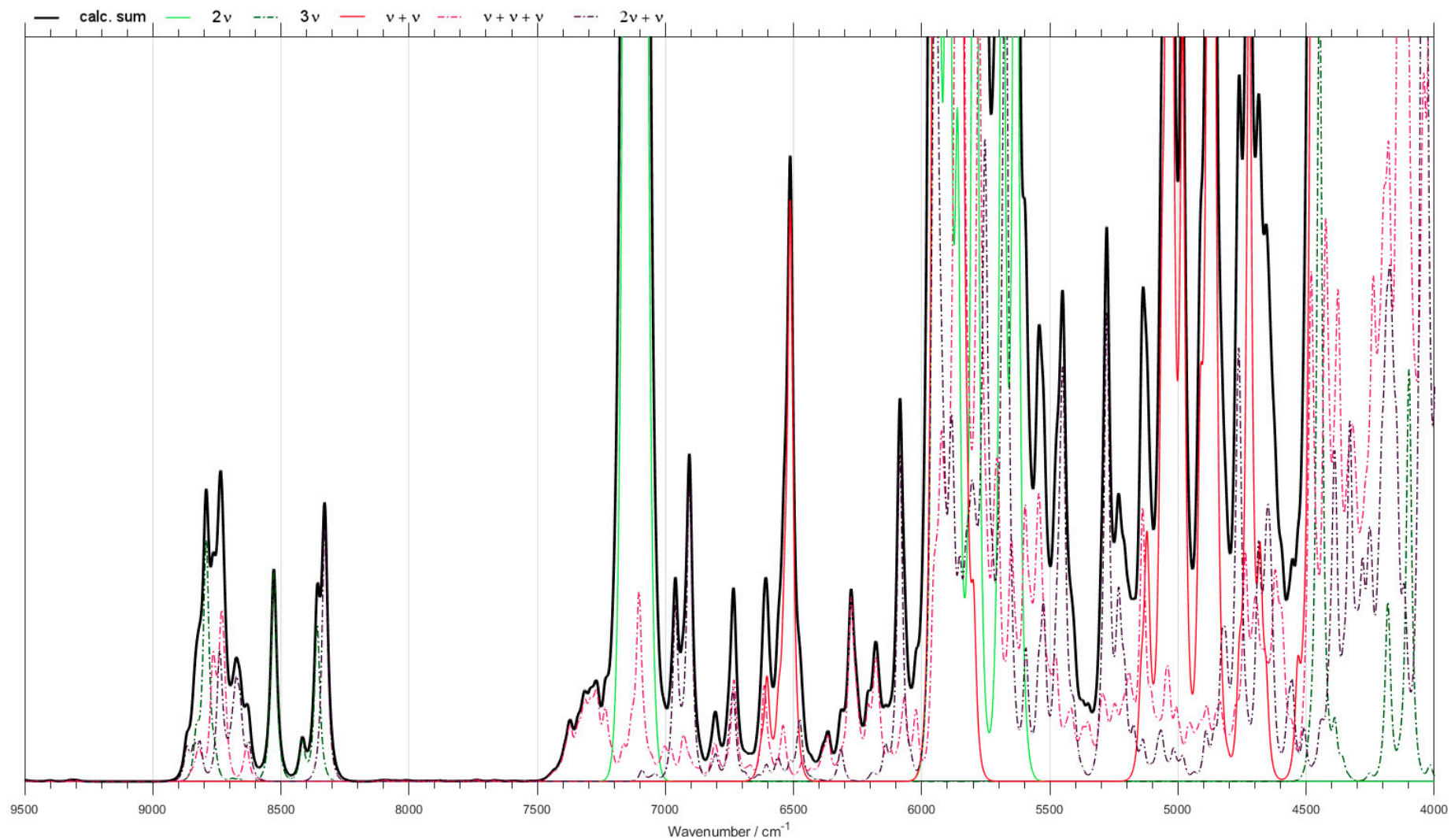


Figure S27. (High-resolution copy of Figure 3) Contributions from minor bands in NIR spectra of $\text{CH}_3\text{CH}_2\text{OH}$ calculated with GVPT2 method at B2PLYP-GD3BJ/def2-TZVP//CPCM level of electronic theory.

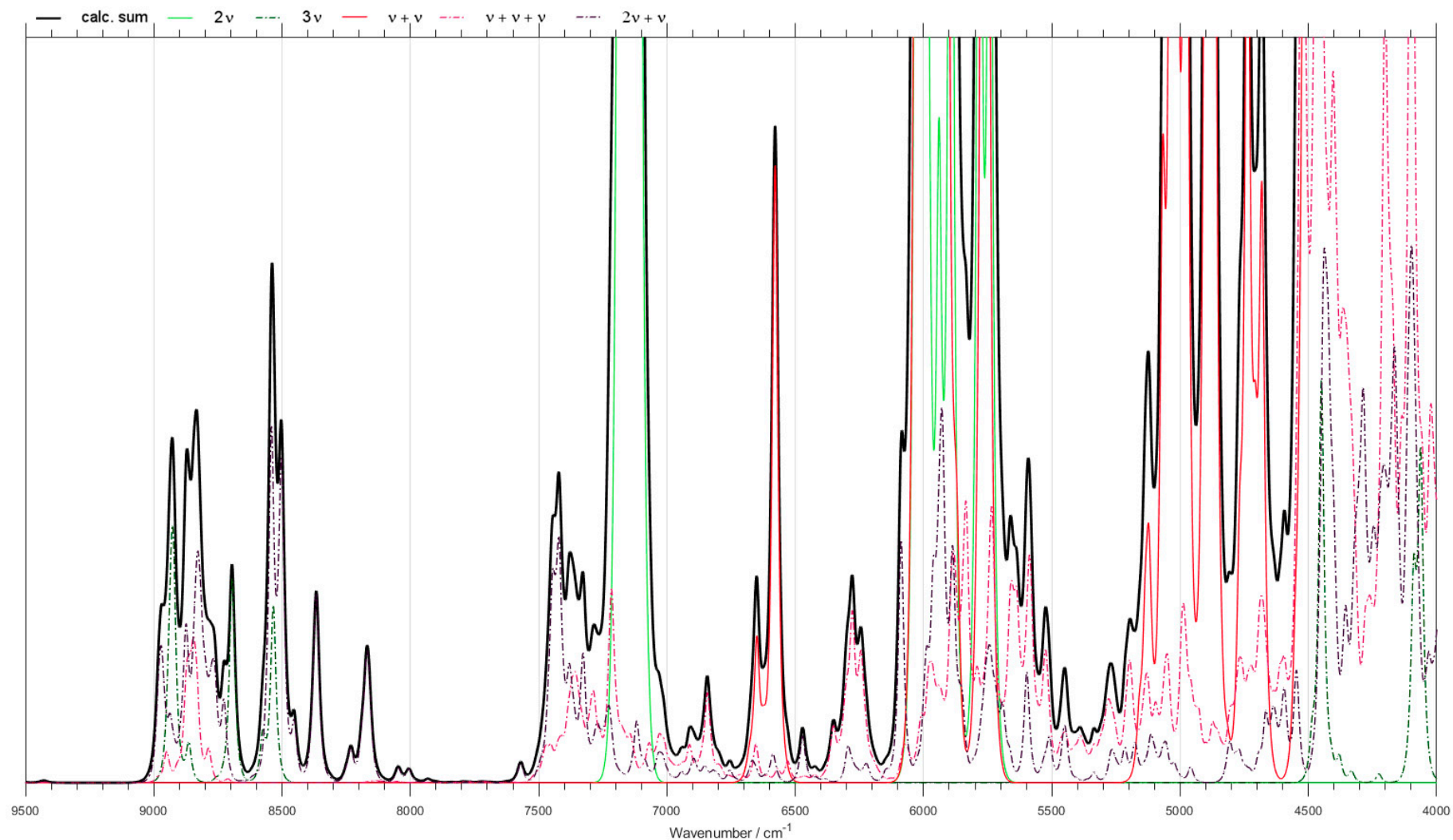


Figure S28. (High-resolution copy of Figure 3) Contributions from minor bands in NIR spectra of $\text{CH}_3\text{CH}_2\text{OH}$ calculated with GVPT2 method at MP2/aug-cc-pVTZ//CPCM level of electronic theory.

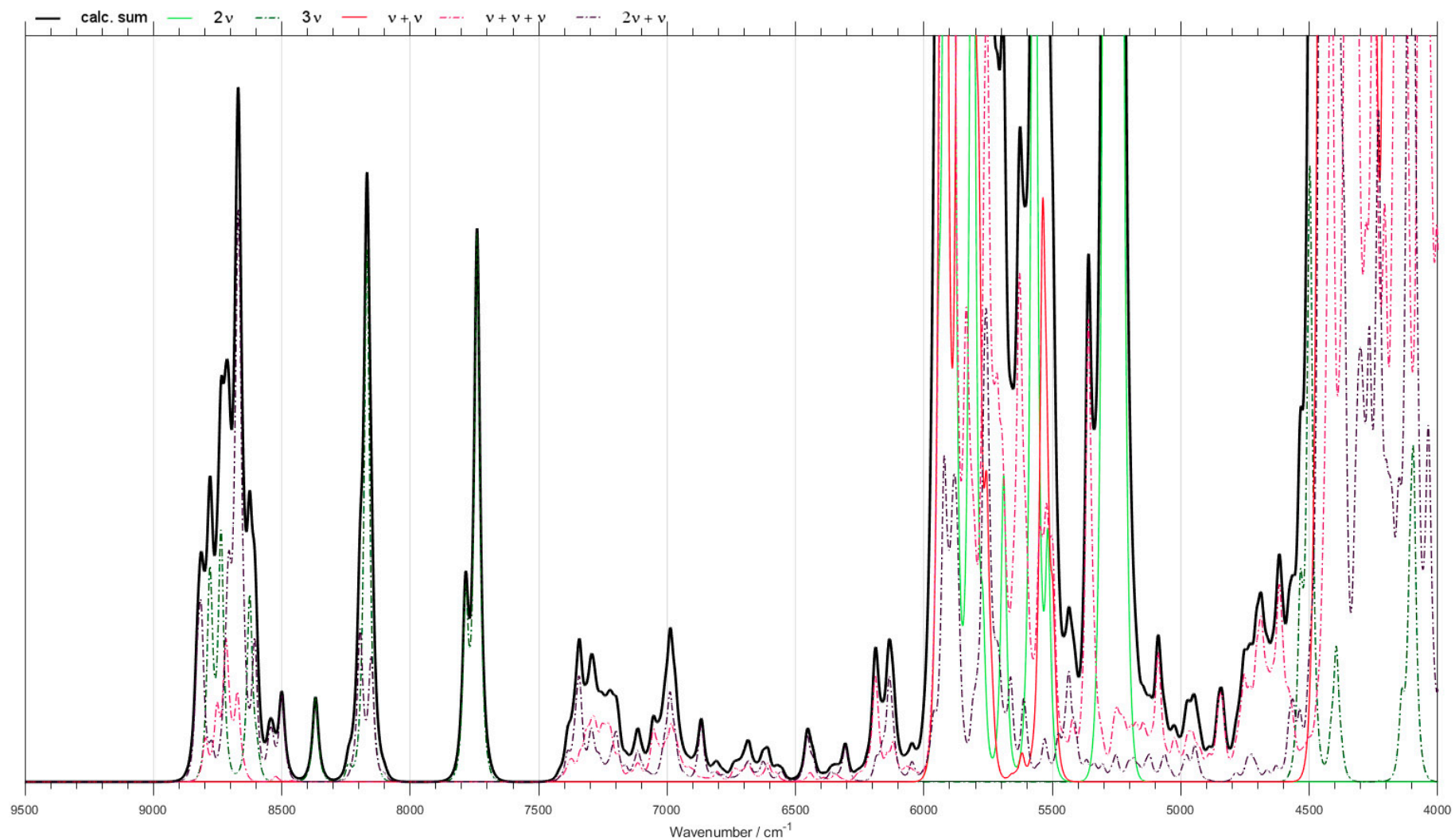


Figure S29. (High-resolution copy of Figure 4) Contributions from minor bands in NIR spectra of $\text{CH}_3\text{CH}_2\text{OD}$ calculated with GVPT2 method at B3LYP-GD3BJ /6-31G(d,p) level of electronic theory.

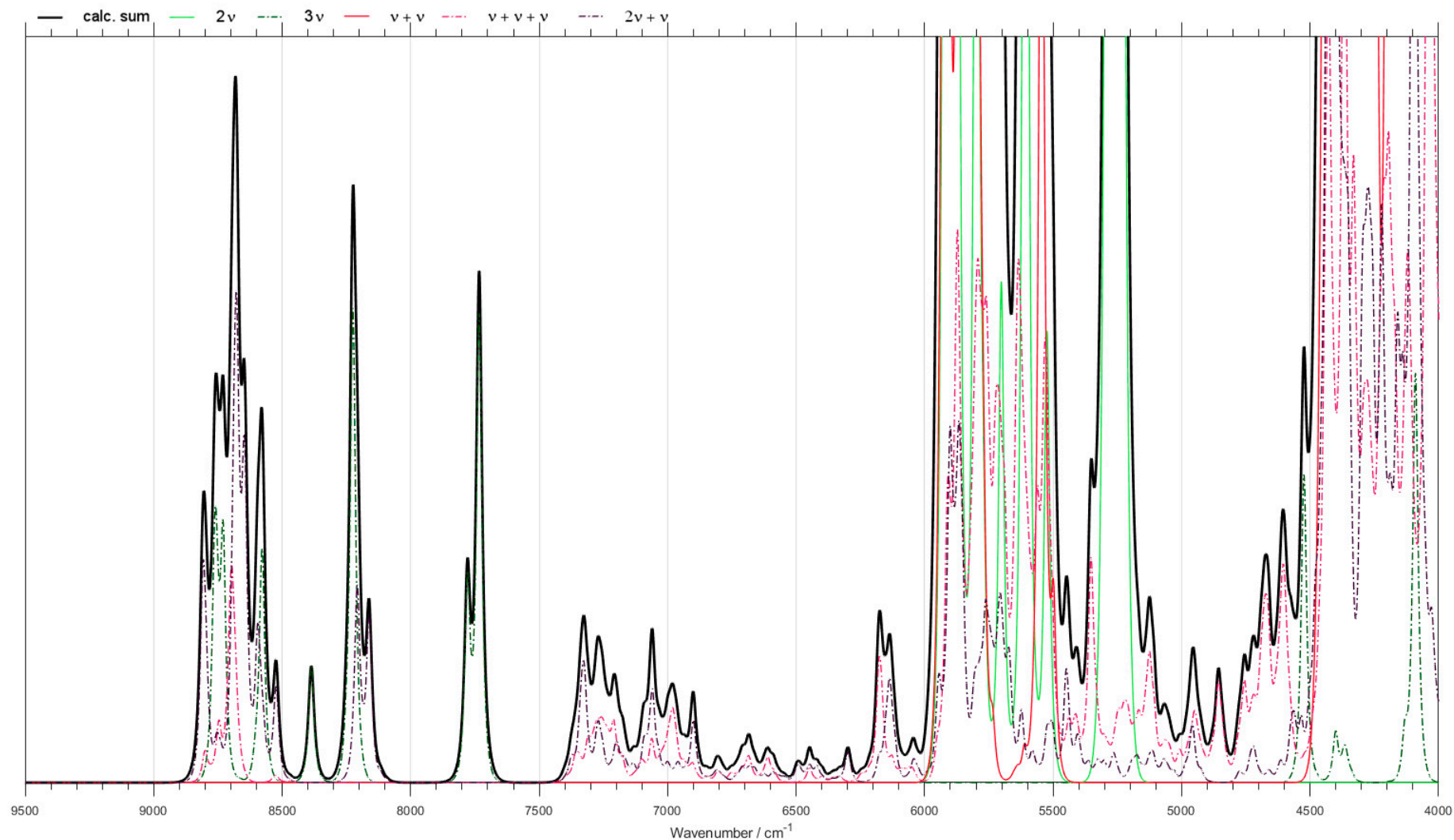


Figure S30. (High-resolution copy of Figure 4) Contributions from minor bands in NIR spectra of CH₃CH₂OD calculated with GVPT2 method at B3LYP-GD3BJ/6-31G(d,p)//CPCM level of electronic theory.

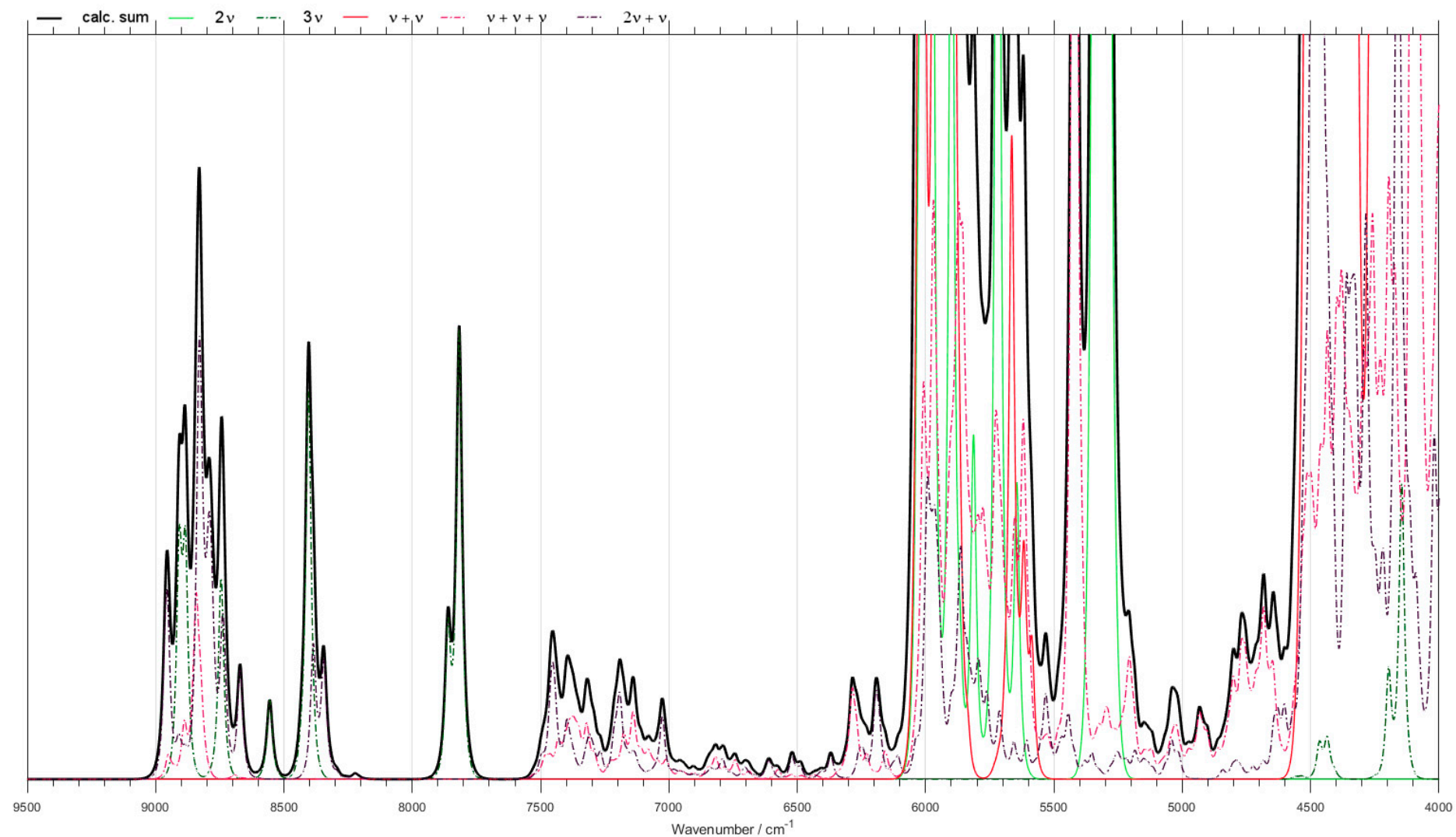


Figure S31. (High-resolution copy of Figure 4) Contributions from minor bands in NIR spectra of $\text{CH}_3\text{CH}_2\text{OD}$ calculated with GVPT2 method at B2PLYP-GD3BJ/6-31G(d,p)//CPCM level of electronic theory.

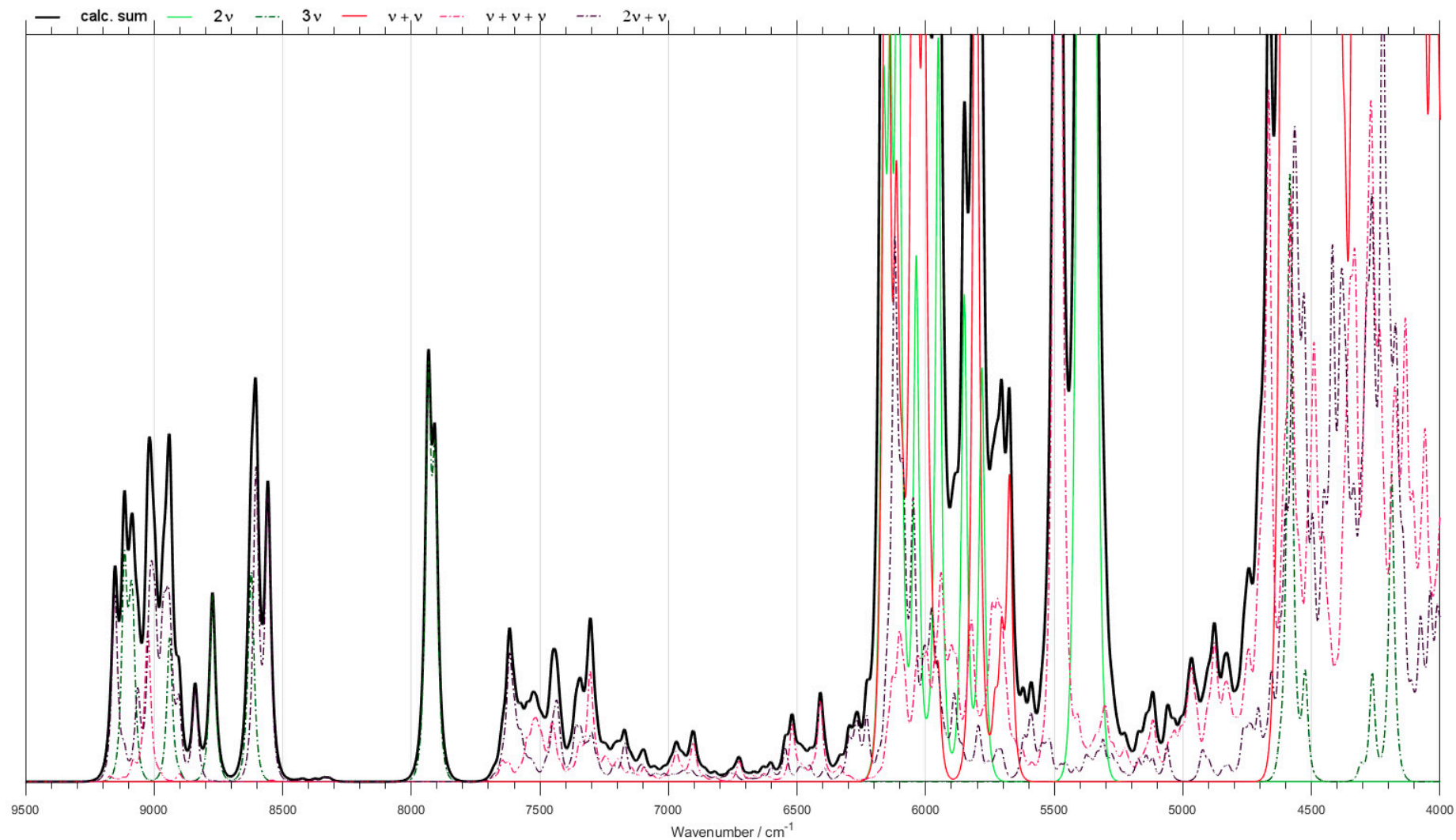


Figure S32. (High-resolution copy of Figure 4) Contributions from minor bands in NIR spectra of $\text{CH}_3\text{CH}_2\text{OD}$ calculated with GVPT2 method at MP2/6-31G(d,p)//CPCM level of electronic theory.

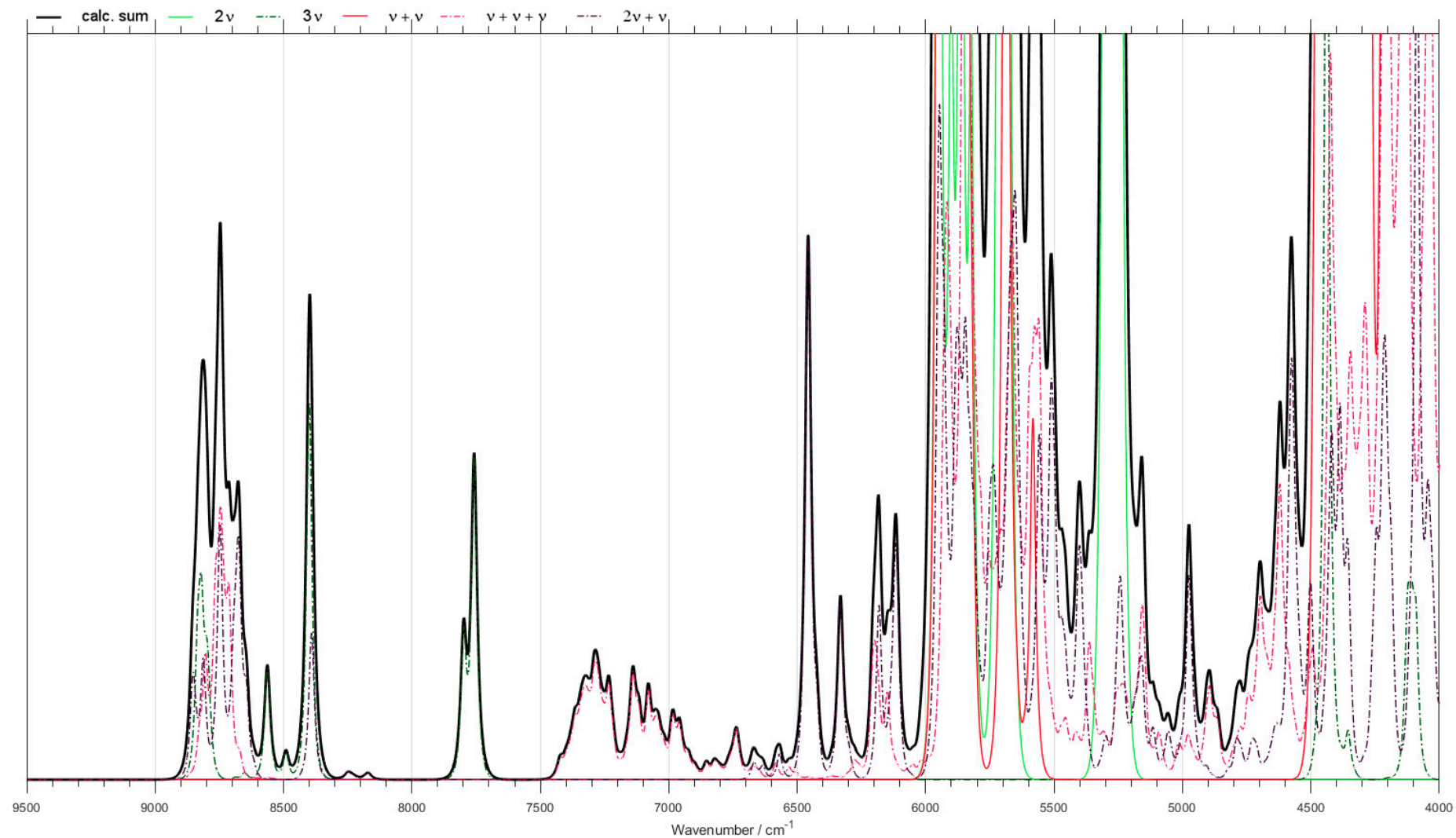


Figure S33. (High-resolution copy of Figure 4) Contributions from minor bands in NIR spectra of $\text{CH}_3\text{CH}_2\text{OD}$ calculated with GVPT2 method at B3LYP-GD3BJ/SNST//CPCM level of electronic theory.

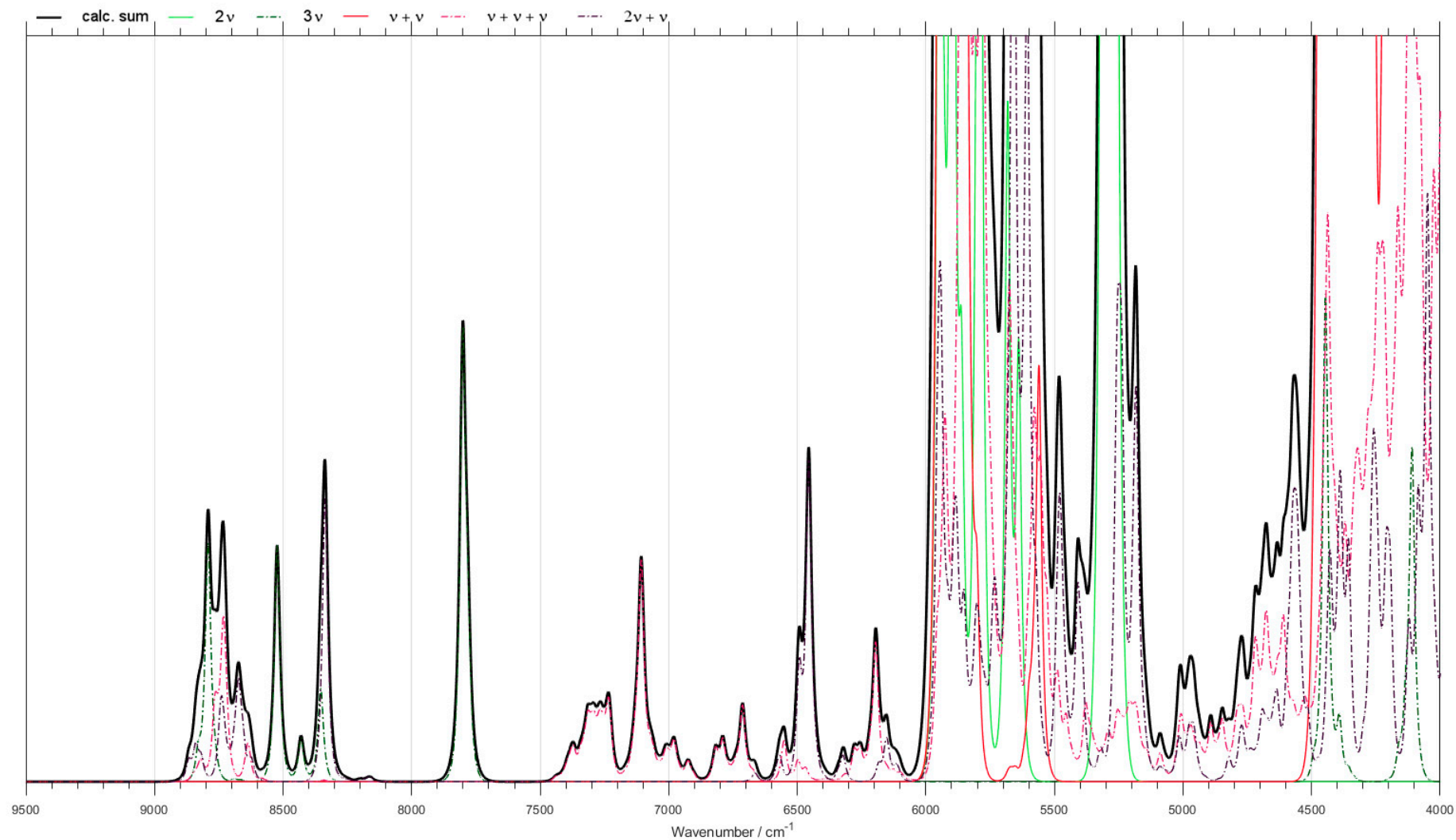


Figure S34. (High-resolution copy of Figure 4) Contributions from minor bands in NIR spectra of CH₃CH₂OD calculated with GVPT2 method at B2PLYP-GD3BJ/def2-TZVP//CPCM level of electronic theory.

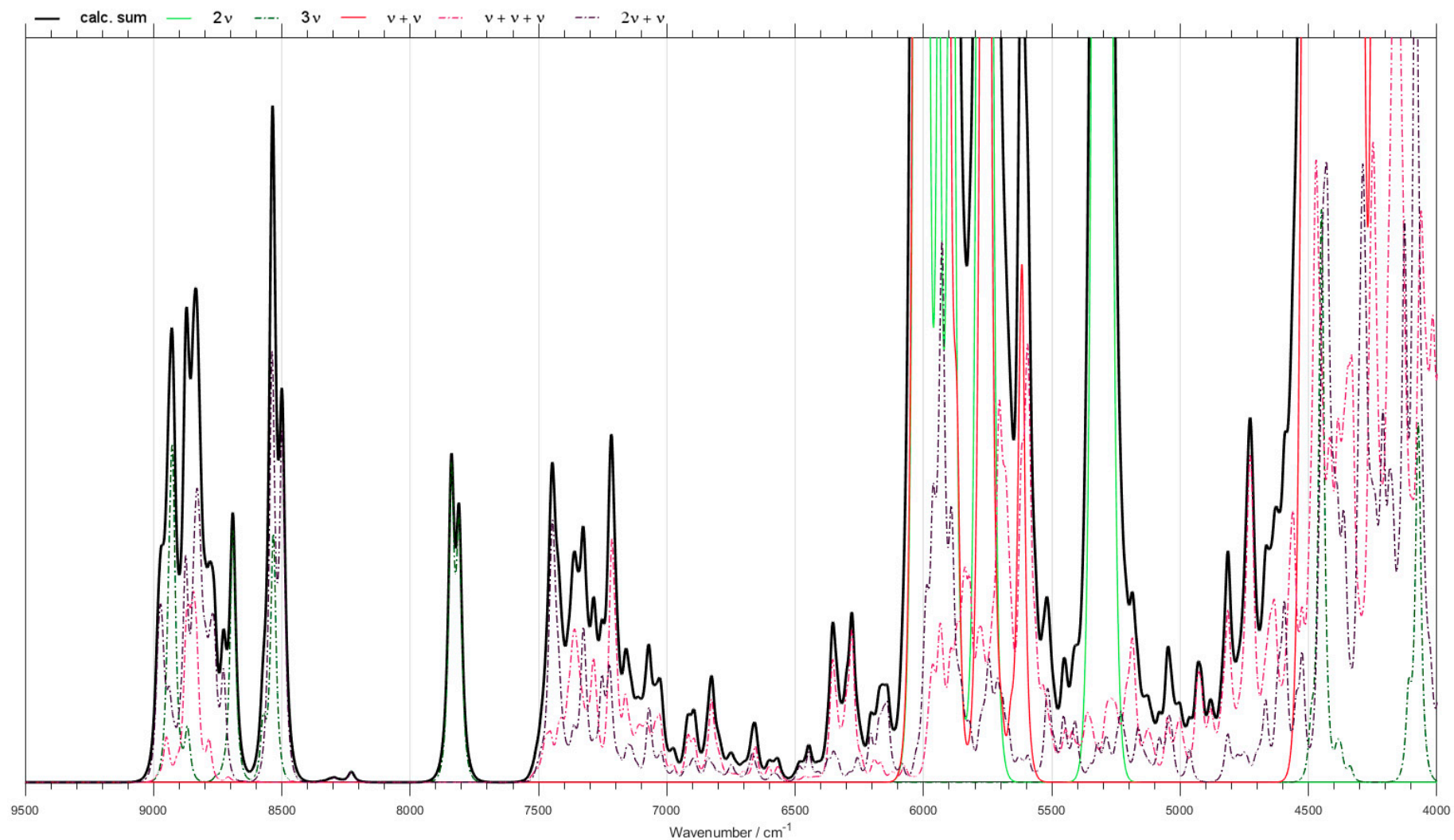


Figure S35. (High-resolution copy of Figure 4) Contributions from minor bands in NIR spectra of $\text{CH}_3\text{CH}_2\text{OD}$ calculated with GVPT2 method at MP2/aug-cc-pVTZ//CPCM level of electronic theory.

II. Tables

Table S1. The relative abundances of gauche (*g*) and trans (*t*) conformers for ethanol isotopomers calculated by different methods.

Conf.		Calculated abundance						
		MP2 /aVTZ +CPCM	B2PLYP-GD3BJ /def2-TZVP +CPCM	B2PLYP-GD3BJ /SNST +CPCM	MP2 /6-31G(d,p) +CPCM	B2PLYP- GD3BJ /6-31G(d,p) +CPCM	B3LYP- GD3BJ /6-31G(d,p) +CPCM	B3LYP- GD3BJ /6-31G(d,p) +CPCM
CH ₃ CH ₂ OH	<i>g</i>	45%	37%	82%	40%	87%	74%	79%
	<i>t</i>	55%	63%	18%	60%	13%	26%	21%
CH ₃ CH ₂ OD	<i>g</i>	48%	24%	73%	46%	78%	76%	79%
	<i>t</i>	52%	76%	27%	54%	22%	24%	21%
CH ₃ CD ₂ OH	<i>g</i>	47%	38%	83%	44%	87%	74%	79%
	<i>t</i>	53%	62%	17%	56%	13%	26%	21%
CD ₃ CH ₂ OH	<i>g</i>	60%	51%	83%	52%	88%	73%	79%
	<i>t</i>	40%	49%	17%	48%	12%	27%	21%
CD ₃ CD ₂ OH	<i>g</i>	58%	51%	84%	54%	87%	73%	79%
	<i>t</i>	42%	49%	16%	46%	13%	27%	21%
CD ₃ CD ₂ OD	<i>g</i>	51%	37%	69%	53%	80%	77%	79%
	<i>t</i>	49%	63%	31%	47%	20%	23%	21%
CH ₃ CD ₂ OD	<i>g</i>	48%	24%	73%	46%	79%	76%	79%
	<i>t</i>	52%	76%	27%	54%	21%	24%	21%
CD ₃ CH ₂ OD	<i>g</i>	50%	35%	70%	52%	80%	77%	79%
	<i>t</i>	50%	65%	30%	48%	20%	23%	21%

Table S2. Potential energy distribution (PED) for *trans* and *gauche* conformers of ethanol (CH₃CH₂OH) based on B2PLYP-GD3BJ/def2-TZVP//CPCM calculations.

trans

ν [cm ⁻¹]	%	Int. coord.	%	Int. coord.	%	Int. coord.	%	Int. coord.	%	Int. coord.
240.08	53%	τ_{CC}	45%	$\delta_{oop}COH$						
282.43	53%	$\delta_{oop}COH$	42%	τ_{CC}						
420.77	78%	$\delta_{sciss}CH_2CO$	12%	$\delta_{rock}CH_3$						
826.43	40%	$\delta_{rock}CH_2$	33%	$\delta_{rock}CH_3$	13%	$\delta_{twist}CH_2$	11%	$\delta_{rock}CH_3$		
904.94	38%	ν_{C-O}	24%	ν_{CC}	21%	$\delta_{rock}CH_3$	7%	$\delta_{rock}CH_3$	6%	$\delta_{wagg}CH_2$
1045.00	49%	ν_{CC}	21%	$\delta_{ip}COH$	14%	ν_{C-O}	8%	$\delta_{rock}CH_3$		
1105.80	54%	ν_{C-O}	22%	$\delta_{rock}CH_3$	8%	$\delta_{rock}CH_3$	5%	$\delta_{sciss}CH_2CO$		

Table S5. Potential energy distribution (PED) for *trans* and *gauche* conformers of ethanol-*d*₃ (CD₃CH₂OH) based on B2PLYP-GD3BJ/def2-TZVP//CPCM calculations.*trans*

ν [cm ⁻¹]	%	Int. coord.	%	Int. coord.	%	Int. coord.	%	Int. coord.	%	Int. coord.
192.63	85%	τ_{CC}	10%	$\delta_{oop}COH$						
266.42	95%	$\delta_{oop}COH$								
376.32	70%	$\delta_{sciss}CH_2CO$	18%	$\delta_{rock}CD_3$	6%	$\delta_{rock}CD_3$				
683.12	48%	$\delta_{rock}CD_3$	23%	$\delta_{rock}CH_2$	16%	$\delta_{rock}CD_3$	9%	$\delta_{twist}CH_2$		
770.55	40%	$\delta_{rock}CD_3$	19%	ν_{C-O}	14%	ν_{CC}	14%	$\delta_{rock}CD_3$		
934.38	34%	ν_{CC}	31%	δ_sCD_3	10%	$\delta_{sciss}CH_2CO$	10%	$\delta_{ip}COH$	9%	$\delta_{rock}CD_3$
1061.99	63%	ν_{C-O}	17%	$\delta_{as}CD_3$	6%	$\delta_{sciss}CH_2CO$	6%	$\delta_{as}CD_3$		
1072.32	72%	$\delta_{as}CD_3$	24%	$\delta_{as}CD_3$						
1090.74	54%	$\delta_{as}CD_3$	18%	$\delta_{as}CD_3$	16%	ν_{C-O}	5%	$\delta_{rock}CD_3$		
1125.48	79%	$\delta_{rock}CH_2$	15%	$\delta_{rock}CD_3$						
1154.80	48%	δ_sCD_3	33%	ν_{CC}	11%	$\delta_{ip}COH$	6%	ν_{C-O}		
1257.45	59%	$\delta_{ip}COH$	25%	$\delta_{twist}CH_2$	6%	ν_{CC}				
1284.71	96%	$\delta_{twist}CH_2$								
1459.15	72%	$\delta_{wagg}CH_2$	15%	$\delta_{ip}COH$	10%	ν_{CC}				
1538.68	95%	$\delta_{sciss}CH_2$								
2197.73	99%	ν_sCD_3								
2320.27	98%	$\nu_{as}CD_3$								
2322.02	98%	$\nu_{as}CD_3$								
3016.88	100%	ν_sCH_2								
3049.95	100%	$\nu_{as}CH_2$								
3821.81	100%	ν_{OH}								

gauche

ν [cm ⁻¹]	%	Int. coord.	%	Int. coord.	%	Int. coord.	%	Int. coord.	%	Int. coord.
204.58	94%	τ_{CC}								
287.82	89%	$\delta_{oop}COH$								
382.13	66%	$\delta_{sciss}CH_2CO$	21%	$\delta_{rock}CD_3$						
677.65	49%	$\delta_{rock}CD_3$	25%	$\delta_{rock}CH_2$	13%	$\delta_{rock}CD_3$	9%	$\delta_{twist}CH_2$		
761.11	40%	$\delta_{rock}CD_3$	20%	ν_{CC}	16%	ν_{C-O}	12%	$\delta_{rock}CD_3$	6%	δ_sCD_3
950.19	33%	δ_sCD_3	28%	ν_{CC}	13%	$\delta_{sciss}CH_2CO$	11%	$\delta_{rock}CD_3$	6%	$\delta_{rock}CD_3$
	6%	$\delta_{ip}COH$								
1038.09	42%	ν_{C-O}	21%	$\delta_{ip}COH$	20%	$\delta_{rock}CH_2$	6%	$\delta_{rock}CD_3$	6%	δ_sCD_3
1073.56	78%	$\delta_{as}CD_3$	11%	$\delta_{rock}CH_2$	7%	ν_{C-O}				
1076.18	69%	$\delta_{as}CD_3$	9%	$\delta_{rock}CH_2$	7%	ν_{C-O}	5%	$\delta_{rock}CD_3$		
1092.43	28%	ν_{C-O}	25%	$\delta_{as}CD_3$	15%	$\delta_{as}CD_3$	14%	$\delta_{rock}CH_2$	13%	$\delta_{rock}CD_3$
1163.57	50%	δ_sCD_3	44%	ν_{CC}						
1247.02	55%	$\delta_{twist}CH_2$	30%	$\delta_{ip}COH$	7%	$\delta_{rock}CH_2$	5%	$\delta_{rock}CD_3$		
1378.71	33%	$\delta_{twist}CH_2$	29%	$\delta_{ip}COH$	27%	$\delta_{wagg}CH_2$	5%	$\delta_{rock}CH_2$		

286.11	91%	$\delta_{oop}COH$								
377.64	66%	$\delta_{sciss}CD_2CO$	20%	$\delta_{rock}CD_3$						
595.93	38%	$\delta_{rock}CD_2$	35%	$\delta_{rock}CD_3$	15%	$\delta_{twist}CD_2$	10%	$\delta_{rock}CD_3$		
744.86	34%	$\delta_{rock}CD_3$	24%	vCC	11%	vC-O	11%	d $\delta_{wagg}CH_2$	11%	$\delta_{rock}CD_3$
	6%	δ_sCD_3								
894.42	38%	$\delta_{twist}CD_2$	24%	$\delta_{rock}CD_2$	15%	$\delta_{ip}COH$	9%	$\delta_{rock}CD_3$		
918.78	17%	vCC	16%	$\delta_{rock}CD_3$	14%	δ_sCD_3	11%	$\delta_{twist}CD_2$	11%	$\delta_{sciss}CD_2CO$
	8%	$\delta_{sciss}CD_2$	7%	vC-O	6%	$\delta_{rock}CD_2$	5%	d $\delta_{wagg}CD_2$		
981.92	48%	vC-O	18%	$\delta_{wagg}CD_2$	12%	$\delta_{twist}CD_2$	7%	$\delta_{sciss}CD_2CO$		
1000.98	29%	$\delta_{twist}CD_2$	25%	$\delta_{rock}CD_3$	22%	$\delta_{rock}CD_2$	12%	$\delta_{rock}CD_3$	5%	vC-O
1076.06	65%	$\delta_{as}CD_3$	31%	$\delta_{as}CD_3$						
1080.46	58%	$\delta_{as}CD_3$	29%	$\delta_{as}CD_3$	7%	$\delta_{sciss}CD_2$				
1097.28	42%	δ_sCD_3	23%	$\delta_{wagg}CD_2$	18%	$\delta_{sciss}CD_2$	7%	vC-O	6%	$\delta_{as}CD_3$
1143.62	57%	$\delta_{sciss}CD_2$	19%	vC-O	7%	$\delta_{wagg}CD_2$	5%	$\delta_{rock}CD_3$		
1206.44	39%	vCC	28%	$\delta_{wagg}CD_2$	16%	δ_sCD_3	14%	vC-O		
1319.55	86%	$\delta_{ip}COH$								
2189.05	96%	ν_sCD_3								
2208.19	95%	ν_sCD_2								
2298.37	55%	$\nu_{as}CD_2$	42%	$\nu_{as}CD_3$						
2310.52	67%	$\nu_{as}CD_3$	29%	$\nu_{as}CD_2$						
2321.35	86%	$\nu_{as}CD_3$	9%	$\nu_{as}CD_2$						
3808.76	100%	νOH								

Table S7. Potential energy distribution (PED) for *trans* and *gauche* conformers of ethanol-*d*₆ (CD₃CD₂OD) based on B2PLYP-GD3BJ/def2-TZVP//CPCM calculations.

trans

ν [cm ⁻¹]	%	Int. coord.	%	Int. coord.	%	Int. coord.	%	Int. coord.	%	Int. coord.
179.69	53%	τ_{CC}	45%	$\delta_{oop}COD$						
204.12	52%	$\delta_{oop}COD$	44%	τ_{CC}						
364.00	70%	$\delta_{sciss}CD_2CO$	17%	$\delta_{rock}CD_3$	6%	$\delta_{rock}CD_3$				
601.58	35%	$\delta_{rock}CD_2$	35%	$\delta_{rock}CD_3$	16%	$\delta_{twist}CD_2$	11%	$\delta_{rock}CD_3$		
751.58	35%	$\delta_{rock}CD_3$	15%	vCC	14%	$\delta_{wagg}CD_2$	13%	vC-O	12%	$\delta_{rock}CD_3$
828.13	56%	$\delta_{ip}COD$	21%	vCC	7%	δ_sCD_3				
928.30	71%	$\delta_{twist}CD_2$	25%	$\delta_{rock}CD_2$						
929.81	27%	vC-O	27%	$\delta_{wagg}CD_2$	11%	δ_sCD_3	10%	vCC	8%	$\delta_{rock}CD_3$
	5%	$\delta_{ip}COD$								
1005.34	38%	$\delta_{rock}CD_2$	33%	$\delta_{rock}CD_3$	17%	$\delta_{twist}CD_2$	11%	$\delta_{rock}CD_3$		
1040.69	37%	vC-O	22%	$\delta_{ip}COD$	19%	$\delta_{sciss}CD_2$	12%	$\delta_{sciss}CD_2CO$		
1074.86	72%	$\delta_{as}CD_3$	24%	$\delta_{as}CD_3$						
1083.27	67%	$\delta_{as}CD_3$	22%	$\delta_{as}CD_3$	6%	$\delta_{sciss}CD_2$				
1104.25	60%	δ_sCD_3	21%	$\delta_{wagg}CD_2$	5%	$\delta_{sciss}CD_2$				

Table S8. Potential energy distribution (PED) for *trans* and *gauche* conformers of CH₃CD₂OD based on B2PLYP-GD3BJ/def2-TZVP//CPCM calculations.*trans*

v [cm ⁻¹]	%	Int. coord.	%	Int. coord.	%	Int. coord.	%	Int. coord.	%	Int. coord.
190.00	89%	$\delta_{oop}COD$	11%	τ_{CC}						
258.77	92%	τ_{CC}								
406.06	77%	$\delta_{sciss}CD_2CO$	11%	$\delta_{rock}CH_3$						
692.37	48%	$\delta_{rock}CD_2$	23%	$\delta_{twist}CD_2$	20%	$\delta_{rock}CH_3$	7%	$\delta_{rock}CH_3$		
852.44	68%	$\delta_{ip}COD$	14%	$\delta_{wagg}CD_2$	10%	ν_{CC}				
867.18	30%	ν_{CC}	26%	$\delta_{wagg}CD_2$	18%	ν_{C-O}	16%	$\delta_{rock}CH_3$	6%	$\delta_{rock}CH_3$
929.51	71%	$\delta_{twist}CD_2$	26%	$\delta_{rock}CD_2$						
988.62	61%	ν_{C-O}	12%	ν_{CC}	10%	$\delta_{ip}COD$	9%	$\delta_{wagg}CD_2$	5%	$\delta_{rock}CH_3$
1083.26	61%	$\delta_{sciss}CD_2$	13%	$\delta_{rock}CH_3$	11%	$\delta_{sciss}CD_2CO$	7%	$\delta_{ip}COD$		
1152.60	50%	$\delta_{rock}CH_3$	17%	$\delta_{rock}CD_2$	16%	$\delta_{rock}CH_3$	9%	$\delta_{twist}CD_2$	6%	$\delta_{as}CH_3$
1187.81	32%	$\delta_{sciss}CD_2$	23%	ν_{C-O}	19%	$\delta_{rock}CH_3$	10%	$\delta_{wagg}CD_2$	7%	$\delta_{rock}CH_3$
1233.96	42%	$\delta_{wagg}CD_2$	33%	ν_{CC}	10%	$\delta_{ip}COD$	7%	ν_{C-O}	5%	$\delta_{sciss}CD_2$
1420.81	88%	δ_sCH_3	10%	ν_{CC}						
1490.98	69%	$\delta_{as}CH_3$	23%	$\delta_{as}CH_3$	6%	$\delta_{rock}CH_3$				
1508.99	68%	$\delta_{as}CH_3$	22%	$\delta_{as}CH_3$	6%	$\delta_{rock}CH_3$				
2191.79	98%	ν_sCD_2								
2266.51	98%	$\nu_{as}CD_2$								
2782.50	100%	ν_{OD}								
3058.30	100%	ν_sCH_3								
3132.15	100%	$\nu_{as}CH_3$								
3133.16	100%	$\nu_{as}CH_3$								

gauche

v [cm ⁻¹]	%	Int. coord.	%	Int. coord.	%	Int. coord.	%	Int. coord.	%	Int. coord.
212.69	96%	$\delta_{oop}COD$								
264.92	93%	τ_{CC}								
412.62	76%	$\delta_{sciss}CD_2CO$	13%	$\delta_{rock}CH_3$						
675.84	56%	$\delta_{rock}CD_2$	16%	$\delta_{rock}CH_3$	14%	$\delta_{twist}CD_2$	7%	$\delta_{rock}CH_3$		
828.91	44%	$\delta_{ip}COD$	38%	$\delta_{twist}CD_2$	11%	$\delta_{rock}CH_3$				
858.49	37%	ν_{CC}	20%	$\delta_{wagg}CD_2$	17%	$\delta_{rock}CH_3$	16%	ν_{C-O}		
976.66	69%	ν_{C-O}	25%	$\delta_{wagg}CD_2$						
1021.81	28%	$\delta_{twist}CD_2$	22%	$\delta_{ip}COD$	12%	ν_{CC}	9%	$\delta_{rock}CH_3$	9%	$\delta_{rock}CH_3$
	8%	$\delta_{rock}CD_2$	7%	$\delta_{sciss}CD_2$						
1068.48	49%	$\delta_{sciss}CD_2$	14%	$\delta_{rock}CH_3$	12%	$\delta_{ip}COD$	9%	$\delta_{twist}CD_2$	8%	$\delta_{sciss}CD_2CO$
1151.99	30%	$\delta_{rock}CH_3$	19%	$\delta_{rock}CH_3$	15%	$\delta_{sciss}CD_2$	14%	$\delta_{rock}CD_2$	7%	ν_{CC}
	5%	$\delta_{twist}CD_2$	5%	$\delta_{as}CH_3$						

